Geomorphology 398 (2022) 108037

Contents lists available at ScienceDirect

Geomorphology

journal homepage: www.elsevier.com/locate/geomorph

DOONIES: A process-based ecogeomorphological functional community model for coastal dune vegetation and landscape dynamics

Bianca R. Charbonneau [a], Adam Duarte [b,c], Todd M. Swannack [d,e], Bradley D. Johnson [d], Candice D. Piercy [d,*]

[a] US Department of Defense Army Engineer Research and Development Center, Oak Ridge Institute of Science and Education, Oak Ridge, TN, USA
[b] USDA Forest Service, Pacific Northwest Research Station, Olympia, WA, USA
[c] Department of Fisheries, Wildlife, and Conservation Sciences, Oregon State University, Corvallis, OR, USA
[d] US Army Engineer Research and Development Center, Vicksburg, MS, USA
[e] Department of Biology, Texas State University, San Marcos, TX, USA

ARTICLE INFO

Article history:
Received 22 February 2021
Received in revised form 20 October 2021
Accepted 5 November 2021
Available online 17 November 2021

Keywords:
Coastal restoration management and conservation
Ecogeomorphology
Plant community dynamics
Storm disturbance

ABSTRACT

In ecogeomorphic systems, such as beach-dune habitats, complex couplings exist between geomorphology and ecology. Abiotic conditions influence vegetation growth and distribution while vegetation imposes a geomorphic feedback, impacting topography. Communities affect storm response by impacting pre-storm state, post-storm recovery, and landscape evolution. Despite their importance, beach-dune and other ecogeomorphic land-sea systems are deteriorating with increased anthropogenic modification and amplified natural disaster impact linked to climate change. A structured approach is needed to develop a more comprehensive understanding of coastal vegetation community interactions with the environment as these interactions underpin topographic change, strom response, and restoration and management efforts. Toward this goal, a spatially explicit process-based grid model, the DOONIES Model, encompassing biological, physiological, and geomorphological drivers of landscape change is presented. DOONIES simulates critical biotic and abiotic processes of vegetation growth, abundance, and spatial distribution dynamics impacting topography and storm response. Biological processes and ecogeomorphic responses are tailored to generalizable dune functional-communities with species-specific representatives. Estimates of the balance between photosynthesis and respiration dictate plant growth and morphology spatiotemporally which in turn impact sediment erosion and deposition. Relative sensitivity analyses indicate that the model is fundamentally driven by the photosynthesis formulation, where parameters such as maximum daily photosynthesis (grams of carbohydrate per day) and light intensity impact vegetation growth. These in turn, indirectly impact topographic change in modeled ecogeomorphic links. DOONIES is standalone and with a biological focus making it unique compared to more physical morphodynamic and hydrodynamic models with which this model is designed to couple. The model was evaluated by comparing simulation topography to actual across 6 years at Island Beach State Park, NJ while modeling Hurricane Sandy and daily wind conditions driving sediment input and output events. The predicted results were within the measurement error for the elevation datasets that the simulations were based on. This new model affords dynamic predictions of the response of naturally occurring and planted dune vegetation communities to typical abiotic conditions, as a tool for supporting and exploring restoration decisions.

1. Introduction

Coastal ecogeomorphic systems have always served vital societal (Stallins, 2006; Viles, 2020) and environmental roles, but these have not always been historically fostered (Jennings, 2004; Jackson and Nordstrom, 2019). Broadly, ecogeomorphic systems maintain an inextricable link between geological and biological processes (Corenblit et al., 2011; Viles, 2020). Landscape and geomorphological processes influence plant community development and distributions, which alter topography and geomorphological processes reciprocally (Stallins, 2006; Corenblit et al., 2011; Viles, 2020). Coastal ecogeomorphic systems provide invaluable ecosystem services, such as supporting diverse and endemic biota, and buffering inland areas from stressors associated with proximity to the ocean (Stallins, 2006; Corenblit et al., 2011; Maun, 2009). Despite inherent instability, coastal areas are highly populated worldwide (Hauer et al., 2016) and in developed settings, there is economic incentive for further investment (Elko et al., 2016; Biel et al., 2017). There is growing interest in shifting away from traditional structural measures for flood risk management to more natural and nature-

* Corresponding author.
E-mail address: Candice.D.Piercy@usace.army.mil (C.D. Piercy).

https://doi.org/10.1016/j.geomorph.2021.108037

based solutions (Schoonees et al., 2019), and with it a renewed interest in understanding and fostering ecogeomorphic links (Jennings, 2004; Harman et al., 2015; Charbonneau, 2015; Feagin et al., 2015; Jackson and Nordstrom, 2019).

Coastal dunes are an ecogeomorphic system that is particularly vulnerable to the effects of climate change (Leatherman et al., 2000; IPCC, 2014, 2019). Storms can naturally reconfigure dune topography (Sallenger, 2000; Houser et al., 2008; Houser and Hamilton, 2009), affecting plant communities that build, stabilize, and recover dunes as ecosystem engineers (Jones et al., 1994; Cheplick, 2016; Charbonneau et al., 2017; Charbonneau, 2019); negatively impacted communities can recover, but they are slow to re-establish such that management efforts emphasize planting vegetation to speed up establishment and jump-start foredune development (Elko et al., 2016; Wootton et al., 2016). Increasing dune vulnerability largely stems from: (1) direct plant mortality and habitat destruction (Spendelow et al., 2002); (2) indirect plant mortality by overwash and breaching (Sallenger, 2000; Houser et al., 2008); (3) a lack of recovery time between storms (Morton and Paine, 1985; Houser and Hamilton, 2009; Durán Vinent and Moore, 2015; Cheplick, 2016); (4) plant community assemblage shifts (Goldstein et al., 2018); and (5) invasive plant establishment (Fei et al., 2014). These cumulative impacts ultimately reduce foredune resiliency in both resisting disturbance and recovering post-storm (Hodgson et al., 2015) whereby the observed global greening of dunes may hyper-stabilize them, but not necessarily reduce their vulnerability to the impacts of climate change (Jackson et al., 2019).

We currently lack a complete understanding of the mechanisms underpinning beach-dune ecogeomorphic feedbacks. Aboveground biomass can enhance sand deposition and foster different topographies (Hacker et al., 2011, 2019; Charbonneau et al., 2021) with plants varying in capture efficiency, morphology, establishment, survival, and density (Hesp, 1984; Hesp, 1989; Zarnetske et al., 2012; Hesp et al., 2019; Charbonneau et al., 2021). Aboveground biomass can also reduce wind and wave erosion (Tanaka et al., 2009; Kobayashi et al., 2013) while belowground biomass concomitantly impacts the latter (Feagin et al., 2015; Bryant et al., 2019). Different plant species and conspecifics vary in root *versus* shoot investment (Charbonneau et al., 2016) and microorganism associations (Forster and Nicolson, 1981; Mardhiah et al., 2016), logically impacting storm response (Charbonneau et al., 2017). Surrounding these feedbacks, the interrelated role of different plant densities and morphologies, pre-storm topography, and sediment dynamics (*i.e.,* transport potential and sediment supply) are less clear (Liu and Singh, 2004; Donnelly et al., 2006; Figlus et al., 2011), but ultimately create a highly heterogenous environment with varying localized storm response (Houser et al., 2008; Davidson-Arnott et al., 2012; Bauer et al., 2012; Charbonneau et al., 2017; Jackson and Nordstrom, 2018).

The need for models that link dune biotic and abiotic dynamics was proposed as early as 1991 (Rastetter) and existing models have explored physical and ecological interactions, but few have approached the system from a photosynthesis-based plant modeling approach. For example, physical processes such as run-up and overwash have been modeled without including vegetation impacts (*e.g.,* van Rijn, 2009; Figlus et al., 2011; Li et al., 2014; Lazarus and Armstrong, 2015). Other models include vegetation impacts on bed shear stress and/or sediment transport by modeling vegetation as percent cover (Baas, 2002; Nield and Baas, 2008; Durán and Moore, 2013; Durán Vinent and Moore, 2015; Keijsers et al., 2016; Roelvink and Costas, 2019), height (Durán and Herrmann, 2006; Luna et al., 2011; Roelvink and Costas, 2019), or density (Rastetter, 1991; de Castro, 1995) with the vegetation parameter changing as a result of mortality (from erosion, burial, or both) and time. These models allow us to test future scenarios relative to physical processes (*i.e.,* sea level rise, storm response, system evolution). However, a process-based vegetation model is needed to allow us to hypothesize and test theories surrounding the ecological and biological interactions that affect the abundance and distribution of communities underpinning these physical processes (Walker et al., 2017; Jackson and Nordstrom, 2019).

The **D**une ec**O**ge**O**morphic vegetatio**N** commun**I**ty photosynth**E**sis-driven **S**patial (DOONIES) model presented here represents the major biotic and abiotic drivers of coastal dune vegetation dynamics. DOONIES is a modular, process-based grid model that simulates plant growth and dune formation though both biotic and abiotic processes including photosynthesis, maintenance respiration, clonal and sexual dispersal, mortality, and associated ecogeomorphic links. These processes impact species-specific functional community distributions, density, and energy allocation, relative to changing above and belowground biomass and associated plant morphometric parameters. The underlying modeling of the incorporated biotic and abiotic relationships are literature-based. The model contains optional simplistic wind and storm prototype sub-models developed to make DOONIES standalone and test the built-in ecogeomorphic interactions encapsulating the biologically and abiotically relevant aspects of vegetation abundance, distribution, and dynamics.

2. Model overview

DOONIES is a stochastic, spatially-explicit, grid-based ecogeomorphic vegetation simulation model incorporating the critical ecological and physiological processes associated with the biotic and abiotic drivers of the life history of coastal dune plants. Model processes and parameters are represented in Fig. 1 and Table 1 and the underlying calculations and relationships encompassing the model are literature-based or theorized based on firsthand field knowledge. The model uses a daily time step to simulate plant growth (grams of carbohydrate day^{-1}) for up to three representative dune vegetation functional communities (1) dune builders (Com_{DB}); (2) burial-tolerant stabilizers (Com_{BTS}); and/or (3) burial-intolerant stabilizers (Com_{BIS}; Woodhouse, 1982; Stallins, 2005; Fig. 2). Growth is modeled as daily biomass change from photosynthesis and respiration, only occurs during the growing season, and varies per community. During the growing season, plants are also able to disperse clonally or by seed. Regardless of season, aboveground biomass impacts aeolian erosion and accretion and mortality can act on all plants, driven by distance to water table (using elevation relative to sea level as a proxy) and ocean, erosion causing uprooting, and burial. The DOONIES grid is initially populated with user-defined vegetation maps or using an algorithm to define niche space.

There are five ecogeomorphic links built into DOONIES: (1) burial increasing photosynthetic vigor of Com_{DB} and Com_{BTS}; (2) changing topographic elevation impacting mortality; (3) burial and (4) erosion impacting mortality; and (5) aboveground biomass impacting deposition and erosion, altering topography. There are simplified and optional storm impact and wind sub-models which were designed to test these ecogeomorphic interactions and prototype integration with physical process models (*e.g.,* the Cross-Shore Numerical Model for which there is an existing built-in coupling (CSHORE; Johnson et al., 2012) or wind transport models like AEOLIS (Hoonhout and de Vries, 2016; Cohn et al., 2019). These sub-models can be turned off and ecogeomorphic links remain for integration with other models.

For the case study presented, default plant parameterizations are primarily empirically estimated from extensive literature review (Supplementary S1) for *Ammophila breviligulata* (Com_{DB}), *Spartina patens* (Com_{BTS}), and *Morella* spp. (Com_{BIS}) (Table 2). They are Mid-Atlantic reference species (Wolner et al., 2013; Huang et al., 2018; Mullins et al., 2019). For computational efficiency, cells represent super-individuals, as each 'individual' represents multiple plants (Scheffer et al., 1995). DOONIES was developed in MATLAB® utilizing the Statistics and Machine Learning Toolbox™ (MathWorks, 2018) and the code is available upon request.

3. Model description

This section is broken into four main sub-sections encompassing (1) model initialization, (2) component descriptions for (a) processes

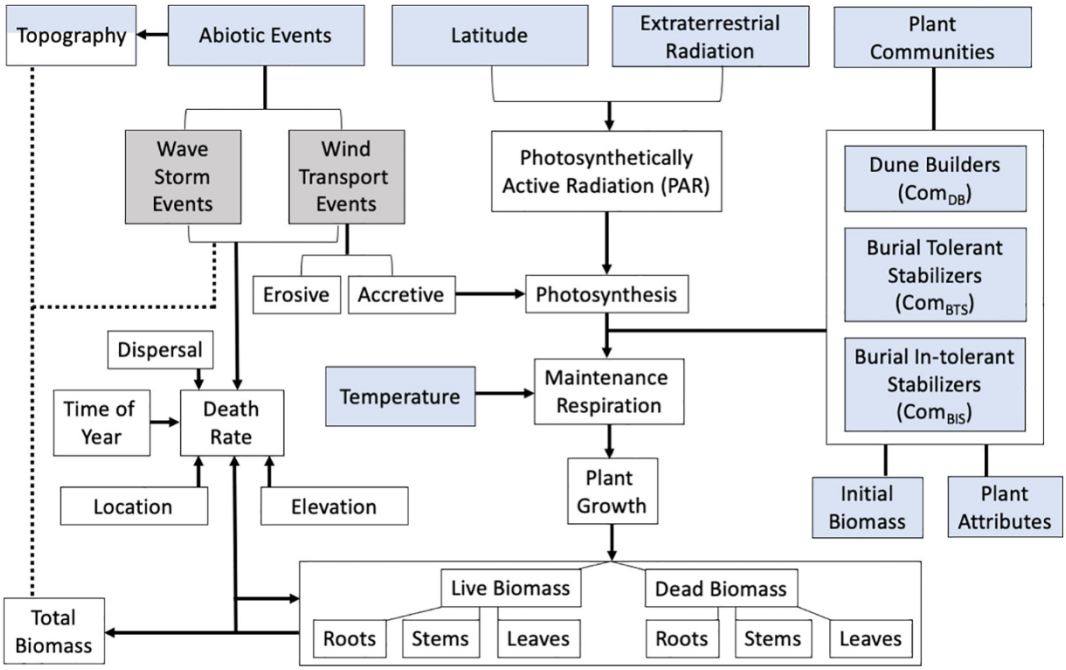

Fig. 1. The conceptual layout of DOONIES. Blue boxes represent input parameters. White and grey boxed both represent model estimates, whereby the grey boxes are estimates explicitly calculated from optional physical sub-models. Solid arrows denote the directional relationships of parameters and estimates. Topography is initially user-provided, then estimated post simulation onset. The dashed line depicts the main ecogeomorphic links of the model which can be met by the optional auxiliary sub-models or by coupling the main elements of DOONIES with other existing models. (For interpretation of the references to colour in this figure legend, the reader is referred to the web version of this article.)

occurring during the growing season, and (b) processes occurring at any time, (3) model evaluation, and (4) model application. Sub-sections reflect details necessary for understanding and using DOONIES.

3.1. Model initialization

3.1.1. Required user input

Site-specific data in Table 3 must be provided as input. The user can also provide initial vegetation distribution grids, otherwise there is a built-in sub-model that initializes communities in the model landscape. If the wind sub-model is used, then site sediment supply must be defined as erosive or accretive.

3.1.2. Model output

Default model outputs per grid cell include total leaf, stem, and root biomass, elevation, occupancy, and morphometrics such as root length, plant height, stem diameter, and plant and stem density. Initial simulation onset conditions are stored as are pre- and post-storm conditions if the optional storm sub-model is used.

3.1.3. Vegetation initial grid population

If community distribution grids are not provided then they are estimated, defined by elevation and distance to the ocean as limiting factors driving distribution. The value of each grid cell for these factors is scaled (between 0 and 1) based on the minimum and maximum values in the model domain. These scaled values are treated as coordinates and used to plot where each community would thrive deterministically in pre-defined habitat space bounds (Fig. 3). Additional heterogeneity is incorporated by 25% of randomly selected suitable cells remaining unoccupied. Vegetated cells are initialized with a random proportion of maximum allowable total biomass (Table 2).

We parameterized and conceptualized where the habitat bounds of each community fell to reflect Com_{DB} and Com_{BIS} having narrower habitat ranges than Com_{BTS} which can occupy both Com_{DB} and Com_{BIS} habitat space (Sharp and Hawk, 1977; Tyndall and Levy, 1978; Moreno-Casasola, 1986; Costa et al., 1996; Cheplick and Demetri, 2000; Uva, 2003; Griffiths and Orians, 2003; Hauser, 2006; Griffiths, 2006; Miller et al., 2008; Young et al., 2011; Mullins et al., 2019). Distance to the ocean and elevation boundaries for Com_{DB} reflect calculated assumed values for the dune toe and beginning of the secondary dune whereby for Com_{BIS} these boundaries are the latter and inland end of a model grid. We derived the location of these habitat features and scaled them from both field measurements and empirical data. There are more details on these calculations and the initialization function in Supplementary S2.

Table 1
The variables in the DOONIES model equations, Eqs. (1) to (11). Variables denoted with * are species-specific parameters (Table 2) that are not calculated by the model. Change in elevation (Δz) is tracked from the beginning to end of a simulation and a growing season.

Symbol	Description	Units
BM	Biomass (dry)	g/cell
BM_{Max}	*Maximum aboveground biomass	g/m^2
D_{St}	Stem density per cell	count
D_{Max}	*Maximum plant density per 0.5 m^2	count
dp	Dispersal potential	–
F	*Fraction of dry matter allocated to each plant part	proportion
G	Glucose requirement for growth of each plant part	g CH_2O g^{-1} dry matter
H_I	*Half-saturation constant for light	µEm^{-2} s^{-1}
k	*Plant tissue light extinction coefficient	–
K	Maintenance respiration cost per plant part	g CH_2O g^{-1} dry matter day^{-1}
P	Instantaneous gross assimilation rate of CO_2	g glucose
P_{Max}	*Maximum daily assimilation rate of CO_2 at 25 °C	g g^{-1} dry matter hr^{-1}
PAR	Daily total photosynthetically active radiation	µE
Q	*Maintenance respiration coefficient at 25 °C per plant part	g CH_2O g^{-1} dry matter day^{-1}
R	Realized maintenance respiration rate	g CH_2O g^{-1} dry matter
R'	Maintenance respiration rate	g CH_2O g^{-1} dry matter
S_D	*Average stem density per plant	count
S_{Max}	*Maximum mass of each plant stem	g
T	Daily mean temperature	°C
$W_{Glucose}$	Daily CO_2 assimilation converted to glucose weight	g CH_2O
Δz	Change in elevation	m

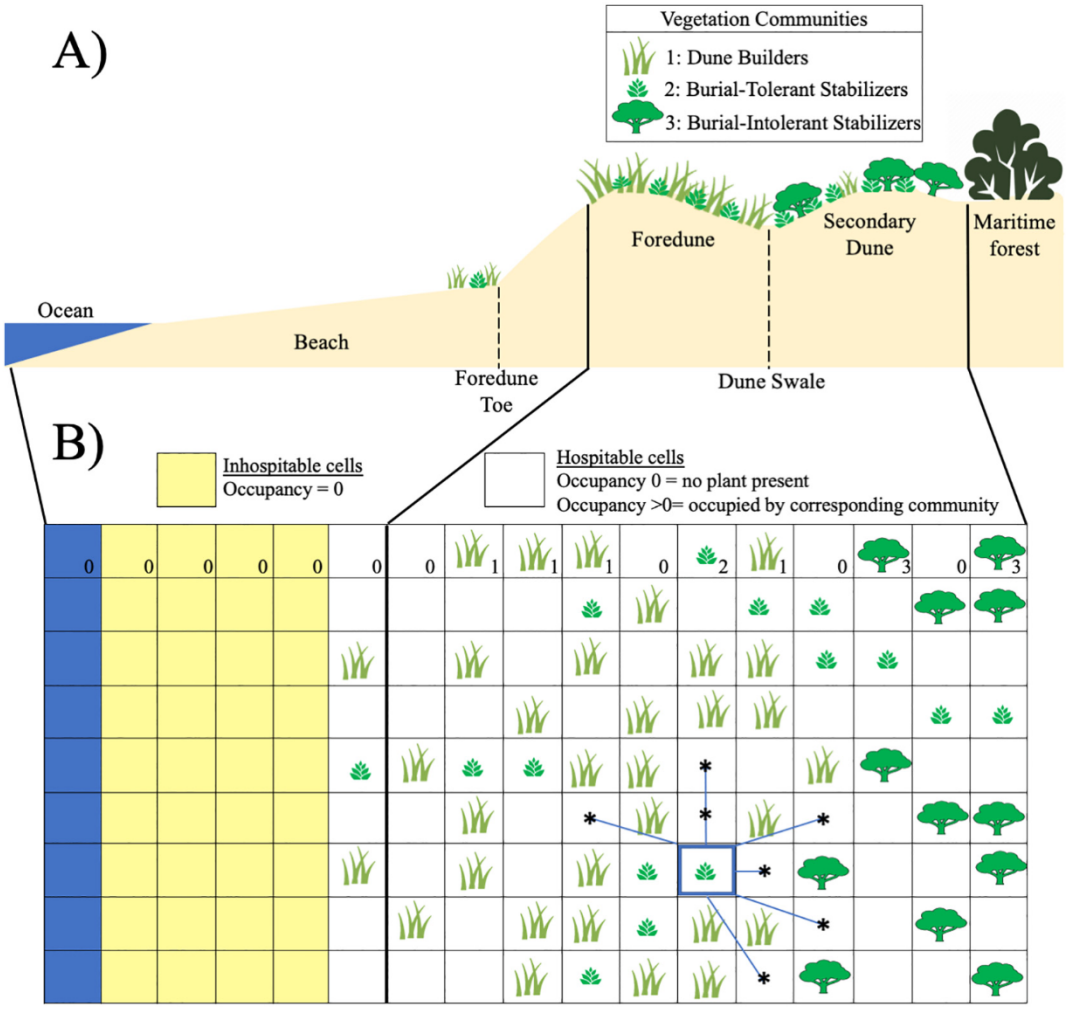

Fig. 2. The coastal dune habitat. (A) A cross section and overhead (B) conceptualization with the three vegetation functional types and their expected relative distributions within the habitat. B) DOONIES is grid-based, and vegetated cells represent super-individuals that can disperse asexually into unoccupied cells within their lateral expansion range.

3.2. Model components: growing season

3.2.1. Photosynthesis

For each community, photosynthesis is calculated during the growing season, from $Season_{Begin}$ to $Season_{End}$ (Table 2). Daily gross photosynthesis is driven by photosynthetically active radiation (*PAR*), calculated using equations from Subroutine ASTRO of Goudriaan and van Laar (1994), and daily total extraterrestrial radiation (imported from Food and Agriculture Organization of the United Nations (FAO), 1998). Intercepted solar radiation (I) is calculated using a van Nes et al. (2003) equation modified for terrestrial species:

$$I = PARe^{-k*BM_{Leaves}} \quad (1)$$

where k is plant tissue light extinction coefficient (Table 1 & 2) and BM_{Leaves} is total leaf biomass (dead & green). A cell must have a minimum leaf biomass, *MinLeaf*, to initiate photosynthesis (Table 2). Daily gross CO_2 assimilation rate is estimated using a three-point Gaussian integration over time (Goudriaan, 1986). Instantaneous gross CO_2 assimilation (P), is calculated with a Hill function from de Wit (1965) based on day length and solar declination morning, midday, and evening:

$$P = P_{Max}\frac{I}{I + H_I} \quad (2)$$

where P_{Max} is the maximum daily CO_2 assimilation (*i.e.*, production) at 25 °C absent any resource limitation, and H_I is the light half-saturation constant (Table 2), the light intensity that photosynthetic rate is ½ P_{Max} (Tables 1 & 2; Mulder and Hendriks, 2014). Daily, gross assimilated carbon is converted to glucose ($W_{Glucose}$) by multiplying it by BM_{Leaves} and $\frac{30}{44}$ (Teh, 2006). Reflecting deposition positively influencing photosynthetic activity in some species, any cells occupied by Com_{DB} and Com_{BTS} maintaining a positive Δz 10 cm or more on a day receive a 5% increase in glucose production (Disraeli, 1984; Yuan et al., 1993; Uva, 2003). The 5% was derived conservatively by examining average increase in leaf area, chlorophyll, and plant height, across successive 5 cm burial treatments (Disraeli, 1984).

3.2.2. Maintenance respiration

The cost of maintenance respiration (R') is defined as the basal rate of metabolism for all processes not resulting in net biomass gain. It is calculated from mean daily temperature and biomass:

$$R' = K_{Leaves}BM_{Leaves} + K_{Stem}BM_{Stem} + K_{Roots}BM_{Roots} \quad (3)$$

where BM terms are green biomass. K terms are maintenance respiration coefficients calculated separately for the leaves, stems, and roots as:

$$K = Q * 2\frac{T - 25}{10} \quad (4)$$

where T is temperature and Q is the respiration quotient, representing the change in respiration rate for a 25 °C change in temperature. Q estimates are from Table 7.1 of Teh (2006). Following Goudriaan and van

Table 2
Plant functional community-specific parameters. Most values are literature-derived from an extensive review of 51 total papers, 27, 18, and 16 for Com_{DB}, Com_{BTS}, and Com_{BIS} respectively. See Supplementary S1 for specific papers used for literature derived and their reported values for parameters.

			Functional vegetation community		
			Dune builders	Burial-tolerant stabilizers	Burial-intolerant stabilizers
			Representative reference species		
Parameter name	Description	Unit	*Ammophila breviligulata*	*Spartina patens*	*Morella pensylvanica & cerifera*
S_D	Average stem density per plant	count	3[c]	4[c]	1[c]
S_{Max}	Maximum mass of each stem	g	1.45[c]	0.65[c]	604[c]
D_{Max}	Maximum plant density per 0.5 m^2	count	17[c]	15[c]	1[c]
	Maximum aboveground biomass (dry)	g/m^2	147.9[c]	78[c]	604[c]
P_{max}	Maximum daily production	$g^{-1}\ h^{-1}$	0.055[a]	0.040[a]	0.05[a]
RL_{Max}	Maximum root length	cm	60[c]	33[c]	50[c]
h_{Max}	Maximum height (tallest leaf tip)	cm	100[c]	75[c]	270[c]
d_{Max}	Maximum stem diameter	cm	–	–	15[c]
C	Stem cross sectional area	cm^2	0.231[c]	0.155[c]	–
r_{RS}	Root-to-shoot ratio	ratio	0.82[a,c]	0.54[a,c]	0.69[a,c]
WintDieOff	Winter root senescence	proportion	0.25[b]	0.25[b]	0.05
MinLeaf	Minimum leaf mass for photosynthesis	Grams	0.5[b]	0.5[b]	0.5[b]
LatExp	# of 0.5 m increments per year	count	8[c]	2[c]	6[c]
$Season_{Begin}$	First day of growing season	ordinal date	45: mid-Mar[c]	105: mid-Apr[c]	46: mid-Feb[c]
$Season_{End}$	Last day of growing season	ordinal date	305: early-Nov[c]	289: mid-Oct	349: mid-Dec[c]
PeakPho	Peak photosynthesis	ordinal date	228: mid-Aug[c]	228: mid-Aug[c]	228: mid-Aug[c]
k	Plant tissue light extinction coefficient	–	0.02[a,c]	0.032[a,c]	0.017[a,c]
H_I	Half-saturation constant for light	$\mu Em^{-2}\ s^{-1}$	9[a]	10[a]	5[a]
F_{lvg}	Biomass allocation to leaves	proportion	0.25[a,c]	0.25[a,c]	0.28[a,c]
F_{stem}	Biomass allocation to stem	proportion	0.30[a,c]	0.40[a,c]	0.31[a,c]
F_{roots}	Biomass allocation to roots	proportion	0.45[a,c]	0.35[a,c]	0.41[a,c]

[a] Calibrated.
[b] Fixed.
[c] Literature derived.

Laar (1994), we account for age affecting respiration by modeling plants with more dead material (*i.e.*, older plants) as requiring less respiration (Gifford, 2003; Teh, 2006; Van Oijen et al., 2010; Thornley, 2011), where realized maintenance respiration rate (R) is calculated daily from R' as:

$$R = R\prime \frac{BM_{Greenleaves}}{BM_{Leaves}} \tag{5}$$

The balance between the cost of maintenance respiration and photosynthetic production determine if biomass and associated morphometrics increase (photosynthesis production > respiration cost) or decrease (respiration cost > photosynthesis production) and by how much among the roots, stems, and leaves.

Table 3
To get started, a user must select (choose a category) and define (input a numeric value) for some site- and simulation-specific parameters.

	User Action Required	Parameter	Unit or details
1	Select	Plant communities included	Com_{DB}, Com_{BTS}, and/or Com_{BIS}
2		Site sediment supply status	accretional or erosional
1	Define	Length of simulation	days
2		Model domain (landscape grid) size	L × W
3		Grid resolution (cell size)	m^2
5		Site latitude	degrees
6		Save step	number of days
1	Provide	Site mean daily minimum air temperature	C° per day, 365 days Jan 1 to Dec 31
2		Site mean daily maximum air temperature	C° per day, 365 days Jan 1 to Dec 31
3		Water level file, such as from tidal station	[a]Any timestep
4		Site elevation: digital elevation model	[a]Beach, dune & offshore

[a] Vertical datums must be internally consistent.

3.2.3. Plant biomass allocation & morphology

Glucose requirement for growth (G_{Growth}) is calculated as:

$$G_{Growth} = F_{Greenleaves}G_{Greenleaves} + F_{Stem}G_{Stem} + R_{Roots}G_{Roots} \tag{6}$$

where F terms represents the fractional allocation of glucose (Table 2) and G terms are glucose requirements for growth (Table 7.4, Teh, 2006). We assume no glucose allocation to flowering or rhizomes, which are not consistently invested in (Maun, 1985), and no clonal integration (*i.e.*, resource sharing) for lack of sufficient data to model (Hester et al., 1994; Charbonneau, 2019). Biomass gain per day (leaf, stem and root) is estimated as:

$$BM_{t+1} = BM_t + F\frac{W_{Glucose} - R}{G_{Growth}} \tag{7}$$

Growth and associated morphological changes are maintained within empirically derived maximum biological limits (Table 2). Maximum green aboveground biomass (BM_{Max}) is calculated as:

$$BM_{Max} = S_{Max}S_D D_{Max} \tag{8}$$

where S_D is average stem density per plant, S_{Max} is maximum stem mass, and D_{Max} is maximum plant density, adjusted to cell size (Table 2). After growth is simulated, green aboveground biomass (BM_{Abg}) is reduced to BM_{Max} if BM_{Abg} exceeds BM_{Max}, with the amount removed from stems and leaves based on F (Table 2). If maximum root biomass (BM_{Max} x root shoot ratio (r_{RS})) is reached, but BM_{Max} is not, then the excess root biomass amount is reallocated to leaf and shoot biomass by F, simulating tillering (Table 2). If green leaf biomass becomes less than *MinLeaf*, then 10% of root biomass is allocated to BM_{Abg} (Best and Boyd, 2001), by F unless root biomass becomes less than *MinRoot*, causing the plant to die (Table 2).

When growth occurs, plant height and root length increase toward maximums, h_{Max} and RL_{Max}, respectively (Table 2; Supplementary S3). Height increase is estimated as h_{Max} divided by half the growing season length, where Com_{BIS} plants also have an annual growth limit

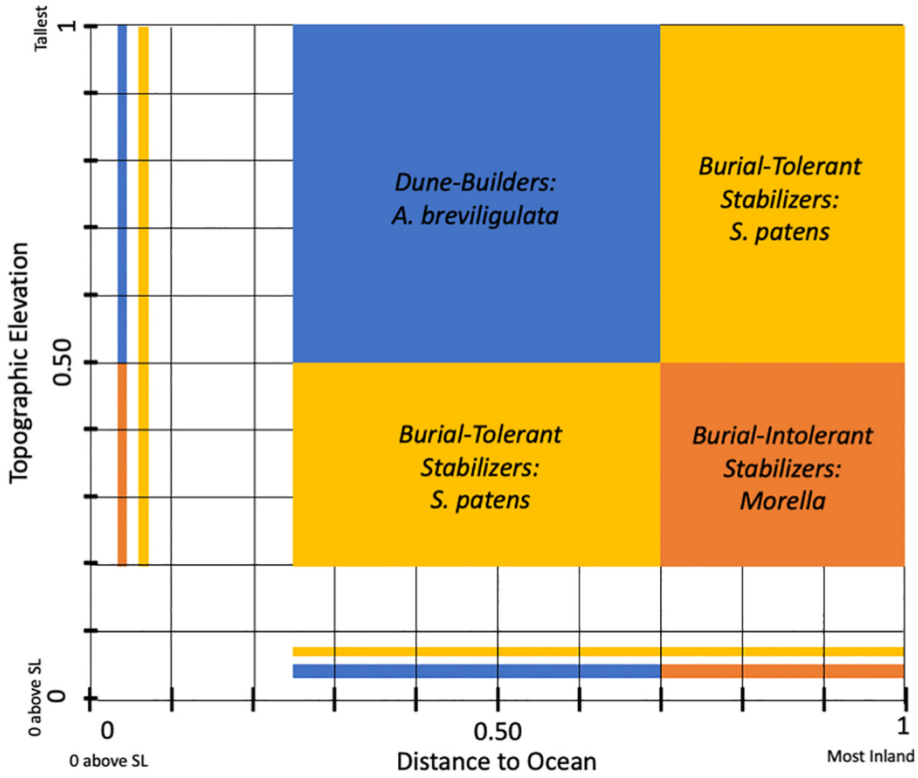

Fig. 3. Vegetation habitat space defined by distance to the ocean and elevation. The specific habitat bounds of Com_{DB} and Com_{BIS} are used to define non-overlapping state space where communities can be established at simulation onsets. For a landscape grid 100 m wide with elevation ranging 0 to 1 m, a cell 30 m from the ocean and 0.6 m tall would be plotted at (0.3, 0.6), falling into Com_{DB} habitat space for establishment.

of 30 cm (Kluepfel and Polomski, 2015). Root length increase is height increase multiplied by r_{RS}. Stem diameter (d) is calculated from height (h) as:

$$Com_{BIS}: d = \frac{h}{h_{Max}} * d_{Max} \tag{10}$$

$$Com_{BD} \text{ and } Com_{BTS}: d = 2 * \frac{C^{0.0005}}{\pi} \tag{11}$$

Stem and plant density are determined from BM_{Abg}. Stems per cell (D_{St}) is:

$$D_{St} = \frac{BM_{Abg}}{BM_{Max}} * St_{Max} \tag{12}$$

where St_{Max} is maximum cell stem density. Plant density is D_{St} divided by S_D, average stem density. Plants in a cell can produce new tillers if the cell has at least 50% maximum root biomass with 20% probability of success randomly in four independent chances at the start of a month June to August (Charbonneau, 2019). Tillering does not cost resources (Maun, 1985).

Com_{DB} and Com_{BTS} biomass and morphology change seasonally reflecting winter die-off and spring emergence. At $Season_{End}$ (Table 2), 20% of BM_{Abg} is reallocated to roots for storage (Busso et al., 1990). BM_{Abg} beyond peak photosynthesis (*PeakPho*) remains over winter as senesced to capture sand in transport events and a proportion of root biomass (*WintDieOff*) is lost over winter to die-off (Busso et al., 1990; Table 2). At $Season_{Begin}$, all senesced BM_{Abg} is removed and 20–30% of root biomass, randomly, is evenly reallocated to leaves and stems.

Seasonality is also built into Com_{BIS}. As semi-evergreen, both roots and stems overwinter. At $Season_{End}$, leaves are removed. At $Season_{Begin}$, 5% of root and 5% of shoot biomass are removed as annual root dieback and branch breakage, and up to 10% of root biomass, randomly, is reallocated to the leaves so photosynthesis can occur. The percentages of dieback for all communities and branch breakage for Com_{BIS} were theorized as conservative estimates given that the authors could not find instances of them having been explored for coastal species.

3.2.4. Dispersal: clonal & seed

Dispersal into new cells is modeled primarily as clonal, reflecting other forms of reproduction being largely unsuccessful and thus considered negligible because of low genetic diversity (Maun, 1985; Slaymaker et al., 2015), seedling survival (Maun, 1985), and seedbank viability and germination (Maun and Lapierre, 1986; Noble and Weiss, 1989; Franks, 2003). There is no parent cell dispersal cost, which loosely incorporates clonal integration defraying resource costs across units (Hester et al., 1994; Charbonneau, 2019).

Dispersal is stochastic and plants can only disperse once a year with two annual dispersal opportunities, mid- and end- of growing season. At mid-growing season, all Com_{BIS}, and all Com_{DB} and Com_{BTS} with ≥50% of BM_{Max} are given an opportunity to disperse. Allowing all Com_{BIS} to potentially disperse accounts for outside bird dispersal and multiple seeds produced per shrub (Hauser, 2006). Cells given a dispersal opportunity have their probability of success drawn from a uniform distribution of pseudorandom integers, 1–100 and dispersal potential (dp) calculated as:

$$Com_{BIS}: dp = \text{1–5 drawn from uniformly distributed pseudorandom integers}$$
$$Com_{DB} \text{ and } Com_{BTS}: dp = \frac{BM_{Abg}}{BM_{Max}} * 100 \tag{13}$$

Cells where dp is greater than dispersal probability will disperse if at least one unoccupied cell is in range of its lateral expansion (*LatExp*; Table 2). Clonal dispersal is only into bare cells as competition is not currently integrated into DOONIES. If there are multiple available cells, then the cell dispersed into is selected randomly. The 1–5% Com_{BIS} success reflects seed germination rates (Fordham, 1983). This process is

repeated at the end of the growing season for cells that did not disperse mid-growing season meeting the aforementioned criteria. New plants emerge with *MinLeaf* for leaf biomass, 10% of maximum aboveground stem weight for stem biomass (S_{Max}), and double the aboveground biomass for root biomass, reflecting younger plants investing more in roots than shoots (Charbonneau, 2019).

To incorporate wrack and seed dispersal, plants can colonize any bare cells or into cells of their functional community daily. The annual probability of seedling and wrack colonization success is 1% (Webb et al., 1984). This is controlled by how the physical conditions in a cell, based on its spatial position and sediment output and inputs to it, affect its cumulative risk of being hospitable *versus* supporting inhospitable conditions that would cause plant mortality. Section 3.3.1 below describes mortality calculations in more detail. Plants that become established (*i.e.*, successfully colonize in this manner) emerge with the biomass noted above.

3.3. Model components: any timestep

3.3.1. Mortality

Mortality is a series of independent logistic functions affecting survivorship over the duration they affect the plants, based on acceptable minimum and maximum elevation relative to sea level (proxy for distance to water table), distance to the ocean, root length/Δz erosion ratio (uprooting), and Δz burial maximum in the form:

$$mortality\ probability = \frac{1}{1 + b_1 \times e^{(-b_2 C)}} \tag{14}$$

where b_1 and b_2 are unknown coefficients fit to literature-derived mortality and plant distribution data and C is the predictor variable of interest. DOONIES employs a binomial risk equation (Vogel and Castellarin, 2017) to determine mortality probability each timestep per occupied cell based on joint risk across the landscape. All plants are subject to mortality. Other mortality sources are assumed negligible (Maun, 2009). Plants may disperse into unsuitable cells and occupied cells can become unsuitable.

When plants die, all biomass is removed and cell occupancy is set to bare. Survival curve coefficients and survival rates (Supplementary S4) are literature derived for distance to water table and ocean (Sharp and Hawk, 1977; Tyndall and Levy, 1978; Doing, 1985; Moreno-Casasola, 1986; Costa et al., 1996; Cheplick and Demetri, 2000; Uva, 2003; Griffiths and Orians, 2003; Hauser, 2006; Griffiths, 2006; Young et al., 2011; Mullins et al., 2019) and burial depth and uprooting (Godfrey, 1977; Martinez and Moreno-Casasola, 1996; Maun, 1998; Maun and Perumal, 1999; Uva, 2003; Lonard et al., 2010; Konlechner et al., 2013). Burial and erosion mortality are determined from a 7-day moving average which reflects their prolonged, not immediate, impact causing death.

3.3.2. Optional wind & wave event sub-models

There are two optional abiotic sub-models, which were used to simulate and test the ecogeomorphic links: one simulates a storm event and the other aeolian transport events. Both are intentional simplifications of the physical forcings and are intended to serve as proxies for integration with more complex physics-based models in the future. The storm sub-model alters vegetation distribution by converting dune to beach cells, representing transgression, killing impacted vegetation, which assume the elevation of the closest pre-storm beach cell. Transgression width is the hindcasted impact of Hurricane Sandy 2012 (Doran et al., 2013) from reference sites scaled to the model domain per profile by beach width. Dune elevation is also altered. More details in Supplementary S5.

The aeolian transport sub-model samples daily wind speed and direction and an event occurs if they meet or exceed thresholds, accounting for rain and sediment supply. Erosion or accretion is simulated based on if the system is defined as erosive or accretive by the user relative to the wind direction. Maximum transport (+/− 0–40 cm) is calculated from wind speed then reduced per cell to determine Δz by: (1) spatial position (decreasing linearly from the crest; Moreno-Casasola, 1986; Davidson-Arnott et al., 2012) (2) BM_{Abg}, modeled positively related to accretion and negatively related to erosion (Eqs. (15) & (16)), and (3) wind direction relative to if the system is defined as erosive or accretive. More details in Supplementary S6. Biomass is treated as linearly related to sediment accretion and retention but inversely in the ecogeomorphic link:

$$\text{Accretion}: \Delta z_A = \Delta z_1 \times \frac{BM_{Abg}}{BM_{Max}} \tag{15}$$

$$\text{Erosion}: \Delta z_A = \Delta z_1 \times \left(1 - \frac{BM_{Abg}}{BM_{Max}}\right) \tag{16}$$

where Δz_A is the actual elevation change to a cell which is calculated from the initial max amount a cell can receive after accounting for position Δz_1.

3.4. Model evaluation

3.4.1. Model calibration

Vegetation parameters were literature-derived, fixed, or calibrated *via* a pattern-orientated approach (Wang et al., 2018; Table 2). Parameters where no data were available, were systematically changed until BM_{Abg} matched realistic natural values compared to BM_{Max}. Literature-derived parameters were calibrated within the range of reported values to produce more realistic BM_{Abg}. For example, the k light extinction coefficients, were literature derived for crop grasses from leaf area indexes (Tahiri and Yasuda, 2006), then calibrated down for dune plants using a reduction of a factor of 10 to reduce BM_{Abg} to below the reported maximum reported biological limits of each community.

3.4.2. Sensitivity analyses

We performed a localized sensitivity analysis to assess which parameters most strongly affect model behavior. We altered one parameter of interest, ±50% and ±20% separately, and observed the response of a target variable, BM_{Abg}, for relative sensitivity to change (*RS*), holding all other values constant (Hamby, 1994; Best and Boyd, 2008). Sensitivity model runs were 30 10-year simulations on a 60 m × 300 m grid of 3 m^2 cells with output saved every 28 days. The *RS* of target variable X with respect to a change in a parameter of interest (*P*) relative to its original value is:

$$RS = \frac{\frac{X_i - X_r}{X_r}}{\frac{P_i - P_r}{P_r}} \tag{17}$$

where i is the value produced from the change in P and r is the original value at reference level (Best and Boyd, 2008). Parameters of interest are P_{Max}, k, *WintDieOff*, and F_{lvg}, because they directly and indirectly impact most modeled relationships where their alteration could have cascading effects on model behavior and output. The response variable of interest, BM_{Abg}, was selected because it affects modeled plant morphometric calculations and elevation change (*i.e.*, dune morphology); it also remains relatively consistent across sandy coastal habitats latitudinally (Barbour and Robicaux, 1976).

3.5. Model application: full model case study

To asses model fit, 30 6-year simulations on a 500 × 500 m landscape grid of 2 m^2 cells of Island Beach State Park (IBSP) 2012 to 2017 were performed (Fig. 4). This period allowed us to test all model components, main and optional. The site is a 17-km micro-tidal sandy barrier island. Precipitation and wind speeds are lowest April–August, when southerly winds predominate (Gares, 1992; NOAA Gauge 8531680). The tested

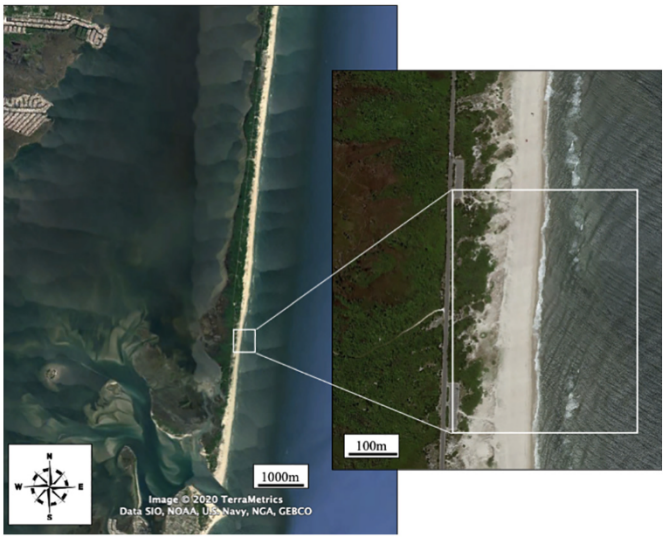

Fig. 4. Case study site. Simulations performed on a 500 m × 500 m stretch of Island Beach State Park, NJ with the road as the inland boundary. 39°47′40.21″N, 74° 5′33.18″W.

section of foredune is dominated by *A. breviligulata* (Com_{DB}). *Spartina patens* (Com_{BTS}), is found bayside in marsh habitat, but less commonly on the dune despite suitable habitat (Martin, 1959). Com_{BIS} is a prominent thicket species as *M. pensylvanica*, landward of the secondary dune (Martin, 1959). Hurricane Sandy (2012) was the most recent major storm to impact the site, causing collision erosion and inundation of the beach and dunes variably across the system (Doran et al., 2013; Charbonneau et al., 2017). The pre-Hurricane Sandy IBSP crest were delineated in ArcGIS™ and ground-truthed with the secondary dune boundary as per Charbonneau et al. (2017), November 2012 (Fig. 5A).

Vegetation distribution and biomass were initialized using pre-Hurricane Sandy LiDAR-derived digital elevation model (DEM) as initial topography (Wright et al., 2014). Placement accuracy was quantified by determining what proportion of Com_{DB} and Com_{BIS} were placed 'correctly', in or seaward of the foredune (defined as bounded by the crest and secondary dune boundary; Fig. 5A & B) and seaward of the secondary dune, respectively. Vegetation initialization is largely deterministic such that this comparison was made once.

Model fit was tested by computing and comparing the sample mean of each cell in the 30 simulations to its known elevation at three periods, T_0 to T_1, T_1 to T_2, and T_3 to T_3:

1. T_0: Initialization (Simulation Day 1, January 1, 2012)
2. T_1: 2012 post-Sandy (Simulation Day 304, November 1, 2012)
3. T_2: 3-yrs post-Sandy, 2015 (Simulation Day 1444, December 1, 2015)
4. T_3: 5-yrs post-Sandy, 2017 (Simulation Day 2086, September 13, 2017)

The corresponding elevation data were from USGS EAARL-B and USACE NCMP, (Wright et al., 2014; OCM Partners, 2020a, 2020b). Resolution on each is <1 m resampled to 2 m with vertical accuracy ±20 cm. Known wind speed and direction data were used with the

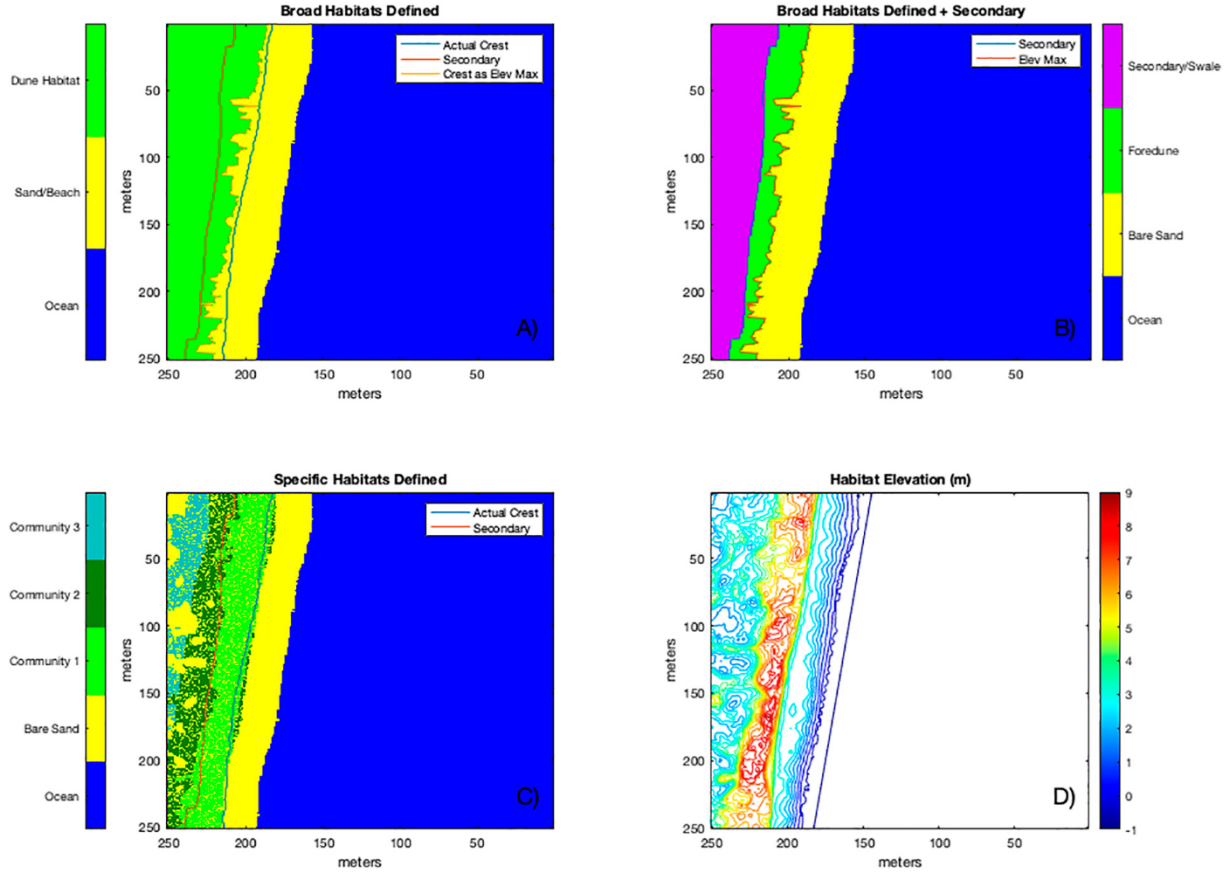

Fig. 5. Island Beach State Park at the simulation onset reflecting vegetation placement by the model and reality. A) The simulation defines the foredune crest as elevation maxima which may tend to be inland of the actual crest, as at IBSP. B) The foredune and swale community at IBSP as defined by the model whereby the secondary dune location was field determined and not information in the model. C) Despite the model not having information regarding sub-habitats in the dune, the transition from Com_{DB} to Com_{BTS} occurs naturally at and around this boundary. On the backshore, seaward of the crest, both Com_{DB} and Com_{BTS} reflect the possiblility for both to act as dune building initiators. D) Non-vegetated dune areas in (C) reflect the lowest landscape elevations.

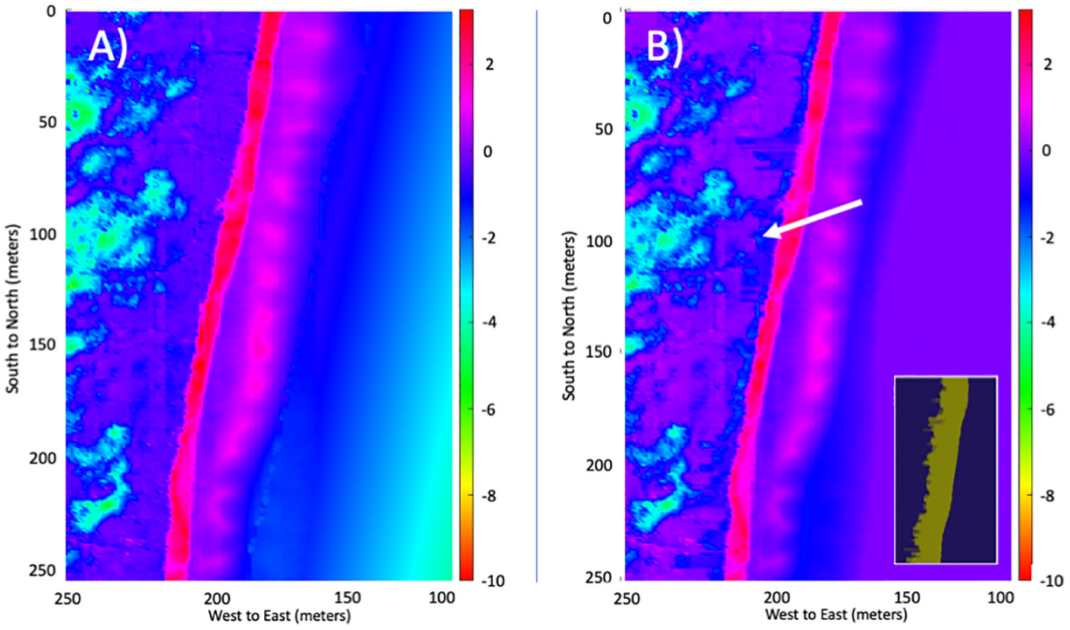

Fig. 6. Case study T_0 to T_1, (A) actual topographic change pre- to post-Sandy (DEM $T_0 - T_1$) *versus* (B) simulation post-Sandy differences ($T_{1Sim} - T_{1Actual}$) (B). Regarding performance, the model over-estimated foredune erosion (too much dune transgression). However, the overall broader erosion patterns regarding swale deepening and beach erosion are congruent with reality, just more conservative in the simulation. Negative values reflect T_0 (A) or T_{1Sim} (B) having lower elevation than in T_1 (A) and $T_{1Actual}$ (B), respectively. Positive values reflect a cell T_0 (A) and T_{1Sim} (B) that was taller pre-storm and eroded in the storm. For orienting, the B inset graph depicts the beach in yellow, and dune and ocean east and west of the beach. *Colorbars to the same scale. The arrow in B denotes the area that was over-transgressed by the storm sub-model T_0 to T_1 which largely lacked vegetation the rest of the simulation. (For interpretation of the references to colour in this figure legend, the reader is referred to the web version of this article.)

wind sub-model and site defined as erosive; differencing the DEMs revealed variations in erosion or accretion between the three periods, but net erosion of the dune as defined from its post-Sandy state T_0 to T_3 (Fig. 6A). Tidal water level data are from NOAA gauge 8,534,720, and temperature data are NOAA NWS daily climatic normals 1981–2010, both for Atlantic City, NJ (https://w2.weather.gov/climate). The storm sub-model was tested, creating initial variability as the pre-storm topography is simulated months ahead of the simulated storm.

3.6. Model application: biological element isolation scenario 1 & 2

Two scenarios were run to isolate the biological elements of the model with baseline conditions more closely aligning with the known state of the IBSP system at scenario onsets. Each scenario is on the same 500 × 500 m IBSP area in the case study in 30 runs performed at 2-m cell resolution. Scenario 1 is T_1 to T_2 (1140 days) and scenario 2 is T_2 to T_3 (642 days). One storm caused some collision erosion (minor compared to Hurricane Sandy <1 m dune transgression) during each period, Hurricane Joaquin T_1 to T_2, and Winter Storm Jonas T_2 to T_3, but dune transport was wind-driven (Dohner et al., 2020) so that the storm sub-model was not included. Vegetation was initialized for both scenarios from the T_1 DEM excluding Com_{BTS}, which was known not to be present; suitable habitat space was shifted to account for this (Supplementary S2, Scenario without Com_{BTS}). After initialization, all vegetation seaward of the known crest location post Hurricane Sandy was removed, reflecting T_1 being immediately following the storm, which eroded vegetation from these areas. This same initial placement was used for scenario 2 as well knowing that Joaquin eroded all or some progradation that might have occurred T_1 to T_2 (Charbonneau et al., 2017; Dohner et al., 2020).

The storm sub-model was not included in either scenario and known wind conditions were used for both. To reflect the known change in the dune elevation observed in this area, the wind sub-model was run as erosive and accretive in Scenario 1 and 2, respectively, testing the ecogeomorphic link between vegetation and transport in both transport scenarios. The topographic change examined in both scenarios is purely a result of the magnitude of wind-driven sediment erosion being dictated by the presence of and production of aboveground biomass which is impacted by the various mortality, dispersal, respiration, and photosynthesis relationships built into the model.

4. Results & discussion

4.1. Vegetation Initialization

DOONIES initialized vegetation in the landscape during the case study reflecting monoculture banded belt communities as observed in nature at IBSP (Maun, 2009; Table 4, Fig. 5C). Com_{DB} thrives in the foredune and backshore, replaced over time by later successional communities in swales and landward (Little and Maun, 1996; Maun, 2009). These patterns are well represented – the foredune is dominated by Com_{DB}, whereas the seaward half of the secondary dune/swale transitions into Com_{BTS}, then Com_{BIS} is prevalent further landward (Table 4, Fig. 5C). Successional patterns have also been re-created in multi-decadal cellular automata simulations for dune plants categorized as colonizers, soil binders, and competitors (Feagin et al., 2005). DOONIES established non-vegetated pockets at the lowest secondary dune elevations (Fig. 5D) these depressions likely represent remnant blowout signatures that have since been colonized by vegetation (Gares, 1992; Charbonneau, 2019). Belted communities might not be formed in landscapes with wider elevation heterogeneity and greater

Table 4
Model initialization placement of dune functional communities. Despite the model only defining the beach and dune habitats broadly and basing placement on elevation and distance to the shoreline, placement was largely appropriate spatially.

Vegetation community	Occupied cells	Backshore	Foredune	Swale/landward of foredune
Dune Builders	4372	36%	54%	10%
Burial-Tolerant Stabilizers	3131	7%	7%	86%
Burial-Intolerant Stabilizers	1578	0%	0%	100%

extremes, warranting more testing. Similarly, testing model behavior for other representations of the functional types outside of the mid-Atlantic region without reparameterization will reveal generalizability and applicability.

4.2. Model sensitivity

Aboveground biomass (BM_{Abg}) is most sensitive, for all functional groups, to changes in the fraction of dry matter allocated to leaves (F_{lvg}), whereby the proportion of root biomass lost over winter to dieoff (*WintDieOff*) is most sensitive only for Com_{BIS}. Changing the *F* of roots, leaves or stems affects the established root:shoot ratio, which is used in many subsequent calculations for morphology and calculating acceptable biological limits as reported in the literature (Supplementary S1). If *F* values are unrealistic or do not sum to one, the built in ecogeomorphic relationships and associated calculations will still function as modeled and intended at all BM_{Abg} beyond the extreme thresholds (*MinLeaf* and BM_{Max}). However, the photosynthetic output, resultant biomass production, and or topographic change will likely be much lower or higher than expected, alerting a user to a potential mis-parameterization. For example, if a user changes F_{lvg} to be extreme (95% as an example) relative to *F* for roots and stems then this high leaf investment will drive up photosynthetic output ultimately allowing more plants to reach their biological limits more quickly and so topographic change will also be accelerated; unrealistic topographic change or extreme BM_{Abg} can thus be a way for a user to identify a parameterization error. Com_{BIS} is more sensitive to reductions in *WintDieOff* than other communities because it is already low normally, 5% stem and root loss. Reducing this further causes Com_{BIS} to reach maximum stem biomass more quickly. Graphs of the relative sensitivity of *k*, *WintDieOff*, and F_{lvg} are in Supplementary S7.

DOONIES is sensitive to changes in the plant tissue light extinction coefficient (*k*) and maximum daily assimilation (P_{Max}) photosynthesis parameters. Increasing or decreasing these parameters too much can cause biomass to reach the biological maximums or mass vegetation die-off. In either scenario, the model loses many aspects of its stochastic nature within four growing seasons, then the relative sensitivity of the parameter decreases (Fig. 7). Over-increasing these parameters causes photosynthesis over-production, driving root stocks to their biological limits across communities within 1–4 years. Once this happens, aboveground biomass plateaus relatively uniformly and annually at the biological limits. Conversely, reducing these parameters too much causes photosynthesis under-production relative to the cost of respiration, creating consistent die-off and a largely unpopulated landscape within 2–4 years. All communities are most sensitive to changes in *k* and P_{Max} in the first few growing seasons because this is when the greatest variability exists in biomass across cells, with fewer extreme outliers. Model behavior for *k* and P_{Max} will remain largely unimpacted until either are reduced or increased enough to largely tip the sensitive balance between photosynthetic output *versus* respiration cost. As a result, fine-tuning *k* and P_{Max} for different sites or species may yield different community distributions and topographies.

Oscillating sensitivity between growing seasons are representative of aeolian sediment deposition events. Fluctuating water levels could also cause this. However, this does not seem to be the case here given that the built-in spatial patterns reflecting deposition and erosion reduction moving inland that have been reported in the literature (Houser et al., 2008; Davidson-Arnott et al., 2012), are reflected in the output. Similarly, oscillating water levels would most affect the species at lower elevations, Com_{BTS} and Com_{BIS} compared to Com_{DB}, but mortality was relatively equal across the communities. There were no other spatial patterns in sensitivity (Supplementary S8). The biomass variability across cells affecting deposition and erosion appears to both reduce uniformity in transport and prevent spatial patterns in *RS* that likely are not apparent in nature.

Future refinements to the photosynthesis algorithm may reduce the sensitivity of model results to *k* and P_{max}. Improving light intensity resolution (*e.g.,* hourly) *versus* daily, could better reflect dynamic conditions (Van der Zande et al., 2010). Incorporating biomass heat stress sensitivity or self-thinning (Gombos et al., 1994; Sharkey, 2005; Ashraf and Harris, 2013) could also limit over-production. Conversely, a more refined age structure could improve respiration costs and better counterbalance photosynthesis, but the literature lacks a reliable correction for this (Gifford, 2003; Teh, 2006) and the lifespan of these plants are unknown, but likely exceed a typical simulation duration of less than 100 years (Treshow and Harper, 1974; Huiskes, 1979). Using size as an age proxy, addresses this issue, but incorporating both age and size could yield better results because the plants maintain type III survivorship (*i.e.,* high initial mortality, high later survivorship) (Chu and Adler, 2014). Lastly, establishing a range of acceptable values for sensitive parameters should limit overall sensitivity and improve output by reducing the deterministic and repetitive cyclical pattern that can emerge if biomass saturates.

4.3. Case study: model application performance

The model under-predicted beach and dune elevation T_0 and T_1, when the storm simulation occurred, by mean −0.35 m, but performance improved as the system recovered post-storm, T_1 to T_2 and T_2 to T_3 when mean difference in modeled and actual dune elevation was 0.18 m and −0.10 m, respectively (Fig. 8; Table 5). Mean difference between the actual and model predicted crest location, used T_0 to T_1 driving the storm simulation was 14.2 ± 8.6 m. The net positive elevation, reflecting simulation under-prediction of erosion at the crest T_2 to T_3 was expected (Fig. 8B) from Hurricane Joaquin and winter storm Jonas collision erosion having occurred in reality, but not having been simulated in the model (Sallenger, 2000; Dohner et al., 2020). Case study elevation differences, simulation *versus* actual, across the dune landscape were within acceptable error for use by coastal managers (Table 5, less than 0.5 to 1 m) and within the vertical accuracy of the elevation datasets used (less than 0.20 m) T_1 to T_2 and T_2 to T_3 (Wright et al., 2014; OCM Partners, 2020a, 2020b).

T_0 to T_1, the storm simulation ultimately over-prescribed transgression, stemming from estimating the crest too landward (Fig. 5A & Fig. 6), resulting in the topography deviating from reality in bands just landward of the true crest by T_1 and T_2 (Fig. 6B & 8A, white arrows). Transgressed areas become denuded in the storm sub-model so the over-transgressed areas that should have been vegetated T_1 to T_3 were not, reducing wind sediment transport to those cells (Fig. 9). Defining the crest remotely using maximum elevation is common (Keijsers et al., 2015; Wernette et al., 2016, 2018) although it can tend to define the feature too landward, as exemplified here and propagated through the output after the storm sub-model was called (Fig. 5 & 9). There is debate on the best method to automate defining the crest (Wernette et al., 2016, 2018; Dohner et al., 2020), and other methods may provide better predictions of crest location.

In 2016 between T_2 and T_3, collision erosion occurred due to extra-tropical cyclone Jonas (Dohner et al., 2020) but was not simulated in DOONIES. By happenstance, the resulting erosion approximated the over-estimation in transgression between T_0 and T_1. It is important to note that these over-transgressed cells drove up the mean and standard error difference between the simulation and actual topographic elevation T_0 to T_1 and T_1 to T_2 (Table 5), whereas vegetated cells landward of the over-transgressed bands aligned more closely with the actual topographic change throughout the full simulation. This occurrence suggests that integration of DOONIES with a morphodynamic or hydrodynamic model incorporating collision erosion and runup from changing water levels would likely more closely reflect reality (Roelvink et al., 2009, 2010; Johnson et al., 2012).

T_0 to T_1 the simulations modeled net erosion despite accretion occurring in reality, regardless of if the model sediment supply was

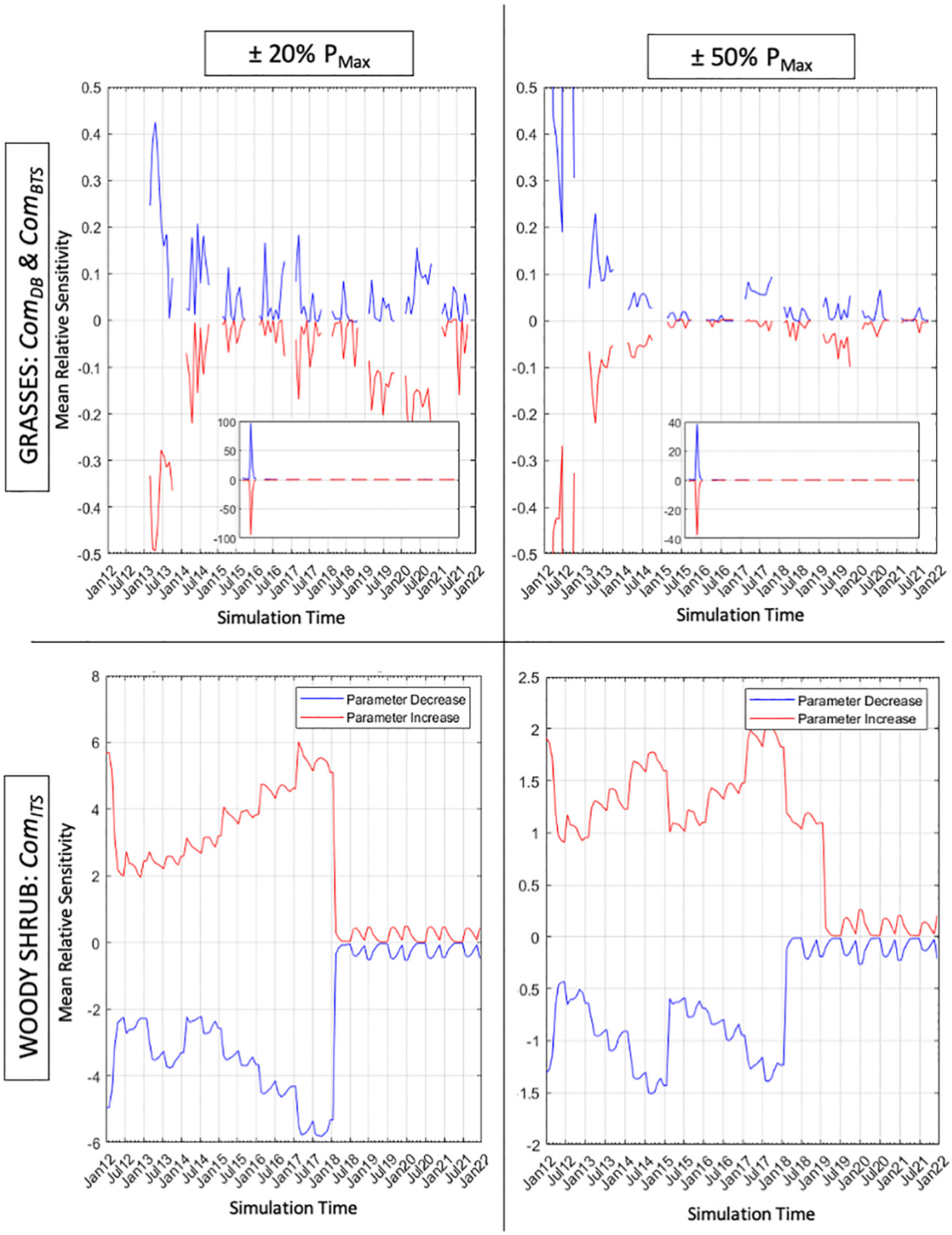

Fig. 7. Relative sensitivity (*RS*) of aboveground biomass (BM_{Abg}) to changes in maximum daily assimilation (P_{Max}). The grasses only have *RS* values during the growing season, reflecting their perennial nature, whereas woody Com_{BIS} maintained *RS* scores greater than 0 throughout the simulation, with stems year-round.

accretive or erosive (Table 5; Fig. 6); this indicates the occurrence of over- prediction of erosion in the 304 days prior to simulating Hurricane Sandy, explicitly from offshore winds which cause erosion regardless of a system being defined as erosive or accretion in the sub-model (Fig. 6B; Supplementary S6). This over-estimation of erosion likely contributed to the storm sub-model performance, supporting models of non-linear systems being sensitive to initial conditions (Baas, 2002). Errors in the wind sub-model likely stem from (1) failing to capture all accretive conditions (Nordstrom and Jackson, 1993; Bauer et al., 2012); (2) the exclusion of near-surface turbulence dynamics (Bauer et al., 2012; Davidson-Arnott et al., 2012); and (3) treating events as mutually exclusive erosive or accretive (Houser et al., 2008; Houser and Hamilton, 2009; de Winter et al., 2015). This sub-model is admittedly simple and was created to test the DOONIES ecogeomorphic links in a more realistic fashion than arbitrarily imposing sediment input and output randomly. Pairing with tested and physically justified transport models such as AEOLIS may fix these issues (Hoonhout and de Vries, 2016; Cohn et al., 2019).

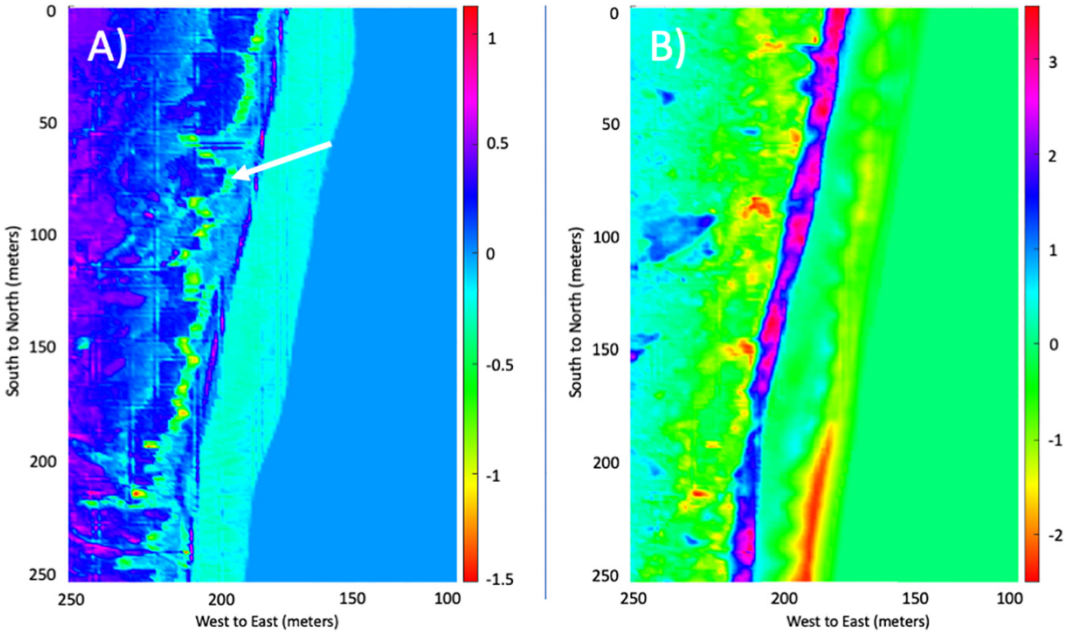

Fig. 8. Case study simulation landscapes (A) T_2,(A) and (B) T_3 (B) compared to the actual topography at the time as $T_{Sim} - T_{Actual}$. Positive and negative values indicate simulation under-estimation of erosion, respectively, compared to reality. (A) From T_1 to T_2, the model agreed well with most dune cells being within ±0.5 m of actual topographic elevation; the arrow denotes the area that was over-transgressed by the storm sub-model T_0 to T_1 which largely lacked vegetation the rest of the simulation. B) T_2 to T_3, the simulated and actual landscapes are more dissimilar as over-erosion occurred across most dune cells while under-erosion occurred in the backshore (deep blue and fuchsia strip). *The colorbars are different between graphs to best reflect the magnitude of elevation difference range. (For interpretation of the references to colour in this figure legend, the reader is referred to the web version of this article.)

4.4. Biological element isolation: scenario 1 & 2 performance

Similar to the case study, in the two scenarios isolating the biological elements in an erosion (T_1 to T_2) and accretion period (T_2 to T_3), simulation *versus* actual elevation differences were within acceptable error for use by coastal managers and within the vertical accuracy of the elevation datasets used (Table 6; Wright et al., 2014; OCM Partners, 2020). Across both full terrestrial landscapes, beach and dune, the model under-predicted the erosion and accretion incurred by 0.38 m and 0.11 m, respectively; this difference is lower than the difference between the actual and simulated topography examined in just the dune and just the vegetated cells, with the exception of examining only the dune as elevation maxima in Scenario 2 (Table 2). This was to be expected as the majority of the beach cells remained unchanged in elevation because they were unvegetated. Bare beach cells (encompassing about 50 cells east to west in the landscape) drive down the mean difference between the actual and simulated topographic change. Simulation and actual topographic difference grow wider when excluding these cells and trying to isolate the dune habitat as elevation maxima, but examining change this way misses vegetated cells landward of this boundary which is predicted too inland (Wernette et al., 2016, 2018). Examining vegetated cells appears to be a better representation of how accurately biomass is modeled as impacting sediment loss and gain and supports the current modeling of the built in and interconnected ecogeomoprphic links which are difficult to isolate here and in nature (Stallins, 2006; Stallins and Corenblit, 2018).

The accretion scenario, scenario 2, better simulated elevation change, within 4 cm of the actual change in vegetated cells, compared to the erosion scenario which under-prescribed erosion by about 0.6 m (Table 6). This could suggest that: (1) the relationship between biomass and sediment retention (erosional scenario 1) *versus* biomass and sediment accretion (accretion scenario 2) may not be equivalent or linear for both (Eqs. (15) & (16)); (2) the wind sub-model under-prescribed erosion instances or amounts in onshore wind events; or (3) both. Treating vegetation as linearly affecting erosion and accretion magnitude is not novel in dune models (*e.g.,* Baas, 2002; Nield and Baas, 2008; Keijsers et al., 2016). These results and previous lab and field studies suggest that a linear relationship between biomass and accretion is appropriately aligned with the literature (Zarnetske et al., 2012; Hesp et al., 2019; Charbonneau et al., 2020). However, less is known about how vegetation retains grains to prevent erosion (Okin, 2008; Lindell et al., 2017) and aeolian erosion magnitudes on vegetated dunes may not be linear and can be lower than associated accretion magnitudes in the same area (Charbonneau, 2019). Gaining a better understanding of how vegetation reduces erosion, wind and wave, is a resource priority that is critical to refining these relationships in this and other models (Donnelly et al., 2006; Walker et al., 2017; Elko et al., 2019). The integration of this model with a wind model (*e.g.,*

Table 5
Standard deviation across terrestrial case study simulation cells and mean differences between simulation and actual elevation across periods. Standard deviation is reported because standard error about all means is ≤0.01 m. Negative values indicate accretion T_X to T_{X+1}. Elevation change actual reflects reality by differencing the DEMs. The dune habitat is defined as representing cells at and landward of elevation maxima.

Time period	Simulation cell STD		Elevation change Actual T_x -T_{x+1}		Elevation difference Simulation$_{Tx+1}$ - Actual $_{Tx+1}$	
	Beach & dune	Only dune	Beach & dune	Only dune	Beach & dune	Only dune
T_0 to T_1	0.03 m	0.04 m	−0.39 ± 0.99 m	−1.08 ± 1.12 m	−0.35 ± 0.84 m	−0.80 ± 1.04 m
T_1 to T_2	0.04 m	0.06 m	0.44 ± 0.91 m	1.11 ± 1.13 m	0.04 ± 0.15 m	0.18 ± 0.17 m
T_2 to T_3	0.05 m	0.06 m	−0.03 ± 0.62 m	−0.22 ± 0.41 m	−0.06 ± 0.62 m	−0.10 ± 0.39 m

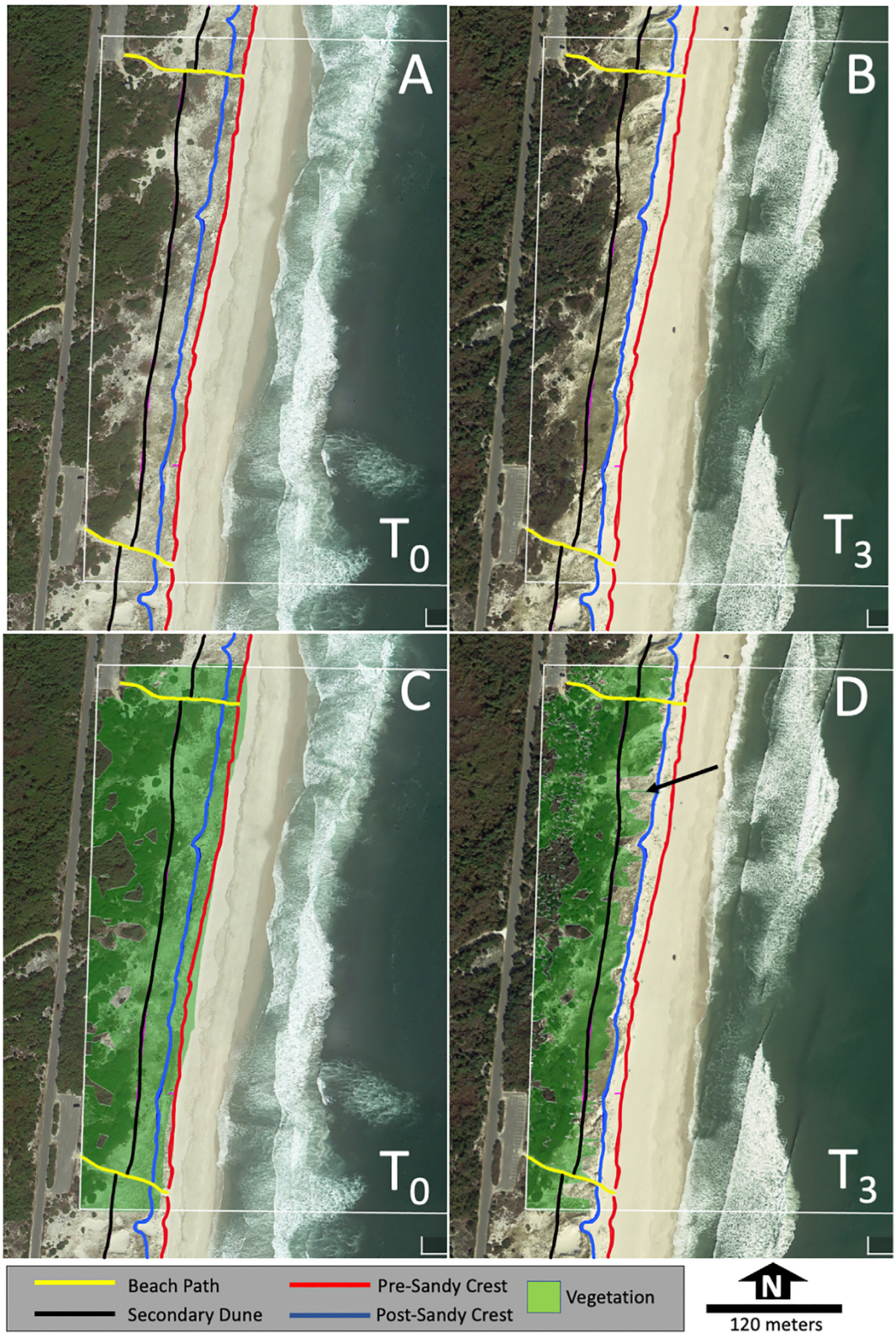

Fig. 9. Vegetation in reality (A & B) *versus* the simulation (C & D) during the full case study duration from T_0 pre-Hurricane Sandy to T_3 5-yrs post-Sandy September 2017. Initial vegetation placement T_0 closely mirrored reality comparing A and C, largely spanning the full dune habitat from the pre-Sandy dune crest landward. At the simulation end (B & D), vegetation remains largely absent between the pre- and post-Sandy crest, except in isolated small patches where dispersal occurred. Denuded areas landward of the pre-Sandy crest where vegetation would be expected in reality stem from over-transgression T_0 to T_1 from the storm sub-model and subsequent slow recovery in re-establishment of vegetation in storm denuded areas. The aerials are projected and pulled from Google Earth View Pro for September 2010 (time soonest T_0 when flight was flown when plants were green and expanded) and October 2017 (one month after actual T_3) reflecting T_0 and T_3, respectively and line layers were mapped in the field (Charbonneau et al., 2017). The arrow in D denotes the area that was over-transgressed by the storm sub-model T_0 to T_1 which largely lacked vegetation the rest of the simulation.

Table 6
Standard deviation across terrestrial scenario 1 and 2 simulation cells and mean differences between simulation and actual elevation across periods. Standard deviation is reported because standard error about all means is ≤0.01 m. Negative values indicate accretion T_X to T_{X+1}. Elevation change actual reflects reality by differencing the DEMs. Elevation differences are examined across the whole landscape, in the dune only (defined as cells at and landward of the elevation maxima), and in cells that were vegetated during the simulation, at its onset or within the simulation, and thus had vegetation affecting accretion and erosion in the ecogeomorphic link. The standard deviation between cells in the three categories on which elevation change is examined were all <0.03 m.

	Elevation change Actual T_x -T_{x+1}			Elevation difference Simulation$_{Tx+1}$ - Actual $_{Tx+1}$		
	Beach & dune	Only dune (Elev Maxima)	Only vegetated (Dune + backshore)	Beach & dune	Only dune (Elev Maxima)	Only vegetated (Dune + backshore)
Scenario 1 T_1 to T_2	0.44 ± 0.91 m	1.06 ± 1.12 m	0.65 ± 1.05 m	0.38 ± 0.98 m	0.99 ± 1.10 m	0.60 ± 1.05 m
Scenario 2 T_2 to T_3	−0.06 ± 0.62 m	−0.26 ± 0.38 m	−0.12 ± 0.55 m	−0.11 ± 0.05 m	−0.05 ± 0.31 m	−0.16 ± 0.53 m

Hoonhout and de Vries, 2016; Cohn et al., 2019) would aid in pinpointing what is driving less accuracy in erosion scenarios to isolate which of the above necessarily coupled causes require further refinement and how (Stallins, 2006; Stallins and Corenblit, 2018).

In both scenarios, vegetation expanded both laterally vis rhizomatous dispersal and to otherwise distant cells in the backshore from simulated seed colonization (Fig. 10). Mortality is treated conservatively in the model, but both plant types colonized cells that were inhospitable through the simulations and were in turn killed by the mortality function. Mortality can be altered by the user to reflect changing conditions. For example, altering water levels to reflect rising sea level scenarios would increase mortality likelihood surrounding distance to the shore (Young et al., 2011; Mullins et al., 2019) and in turn push the hospitable backshore area landward. Conversely, in both scenarios, Com_{DB} expanded seaward, recolonizing space it had held T_0 to T_1, prior to the occurrence of Hurricane Sandy; this occurred at the site as well, as demonstrated by the inset in Fig. 10 showing simulated and actual recovery. The colonization of the backshore in this manner would over time support berm formation and the progradation of the foredune (Hesp, 1984; Hesp, 1989; Maun, 2009; Davidson-Arnott et al., 2012). However, a simulation length of at least seven year would likely be needed to test subsequent berm formation that would arise from plant establishment (Zhang et al., 2015).

4.5. Future coastal dune modeling efforts

DOONIES is a coastal dune model where vegetation is a main driver of ecogeomorphic change; the critical abiotic and biotic processes contributing to inherent system heterogeneity affect vegetation distribution and density and topography. Comparable physically focused models have not explicitly incorporated biological processes affecting vegetation distribution or density/cover metrics beyond erosion and burial, and time impacting cover and mortality (de Castro, 1995; Baas, 2002; Nield and Baas, 2008; Luna et al., 2011; Durán and Moore, 2013, Durán Vinent and Moore, 2015; Roelvink and Costas, 2019). Exceptions to this include Durán and Herrmann (2006), a modified version of the coastal dune model (Moore et al., 2016), and DUBEVEG (Keijsers et al., 2016), which include plant dispersal elements. By comparison, DOONIES incorporates seasonality, mortality, dispersal, photosynthesis, respiration, and plant morphological allometry among root, stem, and leaf biomass distribution. The wide range of morphological and biological parameters calculated should make it compatible to integrate with all existing physical dunes models. These are largely predicated upon a type of percent cover metric and or hydrodynamic models whereby elements of stem diameter of cross-sectional area are a more common metric (Roelvink et al., 2010; Johnson et al., 2012; Roelvink and Costas, 2019).

The reliance of vegetated sand capture on one aboveground biomass metric is not unique to DOONIES (de Castro, 1995; Baas, 2002; Durán and Herrmann, 2006; Nield and Baas, 2008; Luna et al., 2011; Durán and Moore, 2013, Durán Vinent and Moore, 2015; Keijsers et al., 2016; Roelvink and Costas, 2019). The maintenance of consistent topographic gradation stemming from decreasing erosion and accretion crest to inland (Moreno-Casasola, 1986; Davidson-Arnott et al., 2012; Jackson and Nordstrom, 2018), despite cell biomass affecting this otherwise linear spatial relationship (Figs. 6 & 8) supports this. Deposition may be a function of more than one plant biomass metric but using only aboveground biomass encapsulates a lot of the variability surrounding this. Recent wind tunnel tests suggest that plant morphology, in addition to cover or density metrics, also affects this ecogeomorphic link (Hesp et al., 2019; Charbonneau et al., 2021) where their incorporation here and in other models could further improve model results.

The DOONIES multi-community grid populating function can be applied to other models and systems since it is predicated on local topography driving species distributions allometrically. Some coastal dune models contain a generic grass category (Durán and Herrmann, 2006; Luna et al., 2011; Durán and Moore, 2013, Durán Vinent and Moore, 2015). Exceptions include (1) burial- tolerant and -intolerant (Baas, 2002; Keijsers et al., 2016), (2) pioneer grass, mesquite shrub, and shrub (Nield and Baas, 2008), (3) erect herbaceous and stemless (Roelvink and Costas, 2019), and (4) colonizers, soil binders, and competitors (Feagin et al., 2005) categorizations with limited species-specificity in part due to the emphasis on geomorphological responses rather than biological. These communities are initially populated in the landscape with known vegetation cover (Keijsers et al., 2016), estimated from remote sensing surveys (Roelvink and Costas, 2019), or modeled after successional rules requiring multiple generations (Feagin et al., 2005). A grid or profile populating method is largely necessary across models because vegetation distribution data at the landscape level (*i.e.,* beyond transects) are rare (Martin, 1959; Charbonneau, 2019) or inconsistently available at desirable spatial and temporal resolutions (Homer et al., 2015).

Incorporating more vegetation dynamics into modeling efforts has the potential to improve predictions of future response to perturbations and system evolution (Feagin et al., 2015; Elko et al., 2016). A historically incomplete understanding of coastal ecogeomorphic feedbacks combined with concerns that increasing complexity does not necessarily translate to increasing realism have both likely contributed to their limited inclusion in modeling efforts (Murray, 2007; Walker et al., 2017; Jackson and Nordstrom, 2019). Models to date do not reflect the state of the research regarding working to expand or incorporate additional known ecogeomorphic feedbacks (de Castro, 1995; Baas, 2002; Durán and Herrmann, 2006; Nield and Baas, 2008; Luna et al., 2011; Durán and Moore, 2013, Durán Vinent and Moore, 2015; Keijsers et al., 2016; Roelvink and Costas, 2019); however, recent studies have begun to tease apart the nuances of underlying ecogeomorphic coastal feedbacks (*e.g.,* Zarnetske et al., 2012; Feagin et al., 2015; Bryant et al., 2019; Charbonneau et al., 2017; Hesp et al., 2019; Charbonneau et al., 2021). A process-based vegetation model gives us the power to expand the range of future scenarios, natural and managed, tested surrounding the ecological and biological interactions that affect the abundance and distribution of communities underpinning physical processes (Walker et al., 2017; Jackson and Nordstrom, 2019).

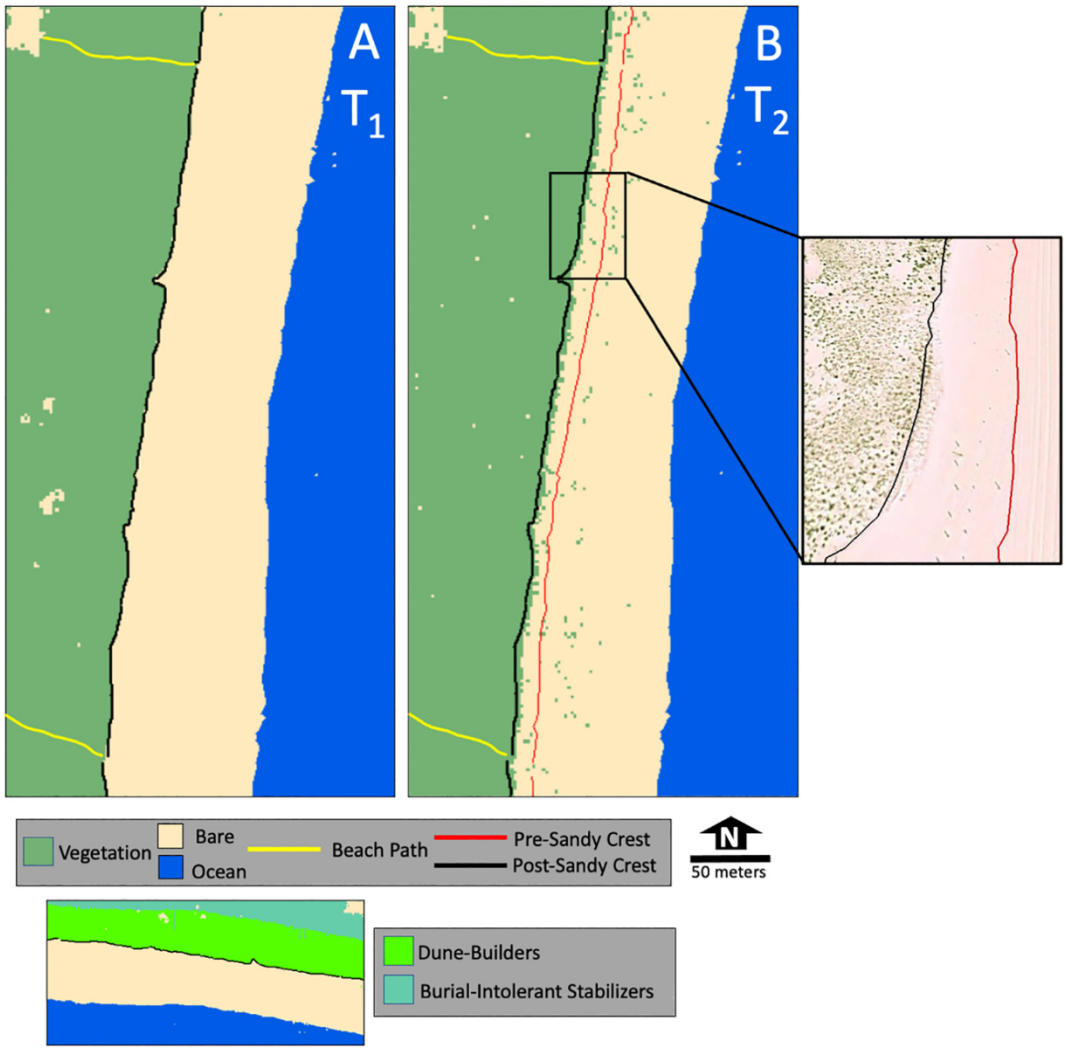

Fig. 10. Vegetation initialization and dispersal in scenario 1 isolating the model biological elements. Vegetation was initialized the same for scenario 1 and 2 (A and small inset), here we show the final state of the landscape T_2 1140 days later (B). Scenario 2 showed the same expansion of vegetation, particularly dune-builders (Com_{DB}) expanding seaward as scenario T_1, but this is less apparent given the simulation duration is nearly half that of Scenario 1. Plants also expanded into open space in the dune habitat and stem density and associated aboveground biomass varied cell to cell (0 to 100% allowable, with associated growth in root biomass) throughout the simulation and growing season reflecting seasonal and inherent heterogeneity and stochasticity in coverage density. Of note, not all cells in the dune were colonized initially or at the end of a scenario as suggested by B, the uniform appearing coverage is a reflection of the resolution. Aerial images from September 2012, pulled from Google Earth View Pro which reflects the historical imagery closest to the T_2 date when the plants were green and fully expanded shows similar expansion where vegetation can be seen spotting the area seaward of the pre-Sandy crest, but to a lesser extent given actual T_2 is 15 months later. (For interpretation of the references to colour in this figure legend, the reader is referred to the web version of this article.)

5. Conclusions/summary

DOONIES is a standalone process-based functional ecogeomorphic community model for coastal dune vegetation incorporating biological, physiological, and geomorphological drivers of landscape change on sandy beach/dune coastlines. Based on the literature-based relationships developed and case study results it is suggested that DOONIES can be applied to a range of sandy coastal locations with different species reflecting the functional communities modeled. DOONIES is designed to be integrated with more complex beach and dune morphology models to hopefully further improve their prediction capabilities by encapsulating drivers of vegetation density and distribution heterogeneity, spatially and temporally. DOONIES is sensitive to changes in photosynthesis parameters and users should consider testing how the light intensity data provided affects biomass production and then adjust P_{Max} and/or k accordingly. The case study showed overall agreement with measured data, testing all ecogeomorphic aspects of the model. Differences in simulation and actual topography across the dune landscape were within acceptable error for use by coastal managers and usually within the vertical accuracy of the elevation datasets used. Storm response and beach-dune evolution models have improved, leading to reduced uncertainty, but were understandably not designed with vegetation in mind as a main driver of change. Integration of these models with DOONIES can expand the range of hypotheses that can be tested surrounding this dynamic habitat. Future model development should incorporate ranges of vegetation parameters to better encapsulate both environmental heterogeneity across communities and reduce the probability of the model becoming deterministic across runs. The ability to simultaneously consider both biotic and abiotic drivers will grow increasingly important as decision-support tools to effectively manage coastal dunes and other ecogeomorphic systems.

Declaration of competing interest

The authors declare that they have no known competing financial interests or personal relationships that could have appeared to influence the work reported in this paper.

Acknowledgments

This study was funded under the Dredging Operations Environmental Reseach and Ecosystem Management and Restoration Research Programs. The use of products or trade names does not represent an endorsement of these products by the authors or the US Departments of Defense, Army, or Agriculture. Any opinions expressed here are those of the authors and not necessarily those of the agencies they represent. The findings and conclusions in this publication are those of the authors and should not be construed to represent any official U.S. Department of Agriculture or U.S. Government determination or policy.

Appendix A. Supplementary data

Supplementary data to this article can be found online at https://doi.org/10.1016/j.geomorph.2021.108037.

References

Ashraf, M.H.P.J.C., Harris, P.J., 2013. Photosynthesis under stressful environments: an overview. Photosynthetica 51 (2), 163–190.
Baas, A.C.W., 2002. Chaos, fractals and self-organization in coastal geomorphology: simulating dune landscapes in vegetated environments. Geomorphology 48, 309–328.
Barbour, M.G., Robicaux, R.H., 1976. Beach phytomass along California coast. Bulletin of the Torrey Botanical Club 103, 16–20.
Bauer, B.O., Davidson-Arnott, R.G.D., Walker, I.J., Hesp, P.A., Ollerhead, J., 2012. Wind direction and complex sediment transport response across a beach-dune system. Earth Surf. Process. Landf. 37, 1661–1677.
Best, E.P.H., Boyd, W.A., 2001. A simulation model for growth of the submersed aquatic macrophyte American wild celery (Vallisneria americana Michx.). ERDC/EL TR-01-5. U.S. Army Engineer Research and Development Center, Vicksburg, Mississippi.
Best, E.P.H., Boyd, W.A., 2008. A carbon flow-based modelling approach to ecophysiological processes and biomass dynamics of Vallisneria Americana, with applications to temperate and tropical water bodies. Ecol. Model. 217, 117–131.
Biel, R.G., Hacker, S.D., Ruggiero, P., Cohn, N., Seabloom, E.W., 2017. Coastal protection and conservation on sandy beaches and dunes: context-dependent tradeoffs in ecosystem service supply. Ecosphere 8 e01791–19.
Bryant, D.B., Bryant, M.A., Sharp, J.A., Bell, G.L., Moore, C., 2019. The response of vegetated dunes to wave attack. Coast. Eng. 152, 103506.
Busso, C.A., Richards, J.H., Chatterton, N.J., 1990. Nonstructural carbohydrates and spring regrowth of two cool-season grasses: interaction of drought and clipping. J. Range Manag. 43, 336–343.
de Castro, F., 1995. Computer simulation of the dynamics of a dune system. Ecol. Model. 78, 205–217.
Charbonneau, B.R., 2015. A review of dunes in today's society. Coast. Manag. 43, 465–470.
Charbonneau, B.R., 2019. From the Sand they Rise: Post-Storm Foredune Plant Recolonization and its Biogeomorphic Implications. Doctoral DissertationUniversity of Pennsylvania, Philadelphia, Pennsylvania.
Charbonneau, B.R., Wnek, J.P., Langley, J.A., Lee, G., Balsamo, R.A., 2016. Above vs. Belowground plant biomass along a barrier island: Implications for dune stabilization. J. Environ. Manag. 182, 126–133.
Charbonneau, B.R., Wootton, L.S., Wnek, J.P., Langley, J.A., Posner, M.A., 2017. A species effect on storm erosion: Invasive sedge stabilized dunes more than native grass during Hurricane Sandy. J. Appl. Ecol. 54, 1385–1394.
Charbonneau, B.R., Nicoletta, R., Wootton, L.S., 2020. A decade of expansion of the invasive plant Carex kobomugi in a coastal foredune system. Biol. Invasions 22, 2099–2112.
Charbonneau, B.R., Dohner, S.M., Wnek, J.P., Barber, D., Zarnetske, P., Casper, B.B., 2021. Vegetation effects on coastal foredune initiation: Wind tunnel experiments and field validation for three dune-building plants. Geomorphology 378, 107594.
Cheplick, G.P., 2016. Changes in plant abundance on a coastal beach following two major storm surges. J. Torrey Bot. Soc. 143, 180–191.
Cheplick, G.P., Demetri, H., 2000. Population biology of the annual grass Triplasis purpurea in relation to distance from shore on Staten Island, New York. J. Coast. Conserv. 5, 145–154.
Chu, C., Adler, P.B., 2014. When should plant population models include age structure? J. Ecol. 102, 531–543.
Cohn, N., Hoonhout, B., Goldstein, E., de Vries, S., Moore, L., Durán Vinent, O., Ruggiero, P., 2019. Exploring Marine and Aeolian Controls on Coastal Foredune Growth using a coupled Numerical Model. J. Mar. Sci. Eng. 7, 13–26.
Corenblit, D., Baas, A.C.W., Bornette, G., Darrozes, J., Delmotte, S., Francis, R.A., Gurnell, A.M., Julien, F., Naiman, R.J., Steiger, J., 2011. Feedbacks between geomorphology and biota controlling Earth surface processes and landforms: a review of foundation concepts and current understandings. Earth Sci. Rev. 106, 307–331.
Costa, C., Cordazzo, C.V., Seeliger, U., 1996. Shore disturbance and dune plant distribution. J. Coast. Res. 12, 133–140.
Davidson-Arnott, R.G.D., Bauer, B.O., Walker, I.J., Hesp, P.A., Ollerhead, J., Chapman, C., 2012. High-frequency sediment transport responses on a vegetated foredune. Earth Surf. Process. Landf. 37, 1227–1241.
Disraeli, D.J., 1984. The effect of sand deposits on the growth and morphology of Ammophila breviligulata. J. Ecol. 72, 145–154.
Dohner, S.M., Pilegard, T.C., Trembanis, A.C., 2020. Coupling traditional and emergent technologies for improved coastal zone mapping. Estuar. Coasts 1–23.
Doing, H., 1985. Coastal fore-dune zonation and succession in various parts of the world. Vegetatio 61, 65–75.
Donnelly, C., Kraus, N., Larson, M., 2006. State of knowledge on measurement and modeling of coastal overwash. J. Coast. Res. 22 (4), 965–991.
Doran, K.S., Stodkdon, H.F., Sopkin, K.L., Thompson, D.M., Plant, N.G., 2013. National assessment of hurricane-induced coastal erosion hazards: Mid-Atlantic Coast. U.S. Geological Survey. Open_File Report 2013-1131 28 p.
Durán, O., Herrmann, H.J., 2006. Vegetation against dune mobility. Phys. Rev. Lett. 97, 188001.
Durán, O., Moore, L.J., 2013. Vegetation controls on the maximum size of coastal dunes. Proc. Natl. Acad. Sci. 110, 17217–17222.
Durán Vinent, O., Moore, L.J., 2015. Barrier island bistability induced by biophysical interactions. Nat. Clim. Chang. 5, 158–162.
Elko, N., Brodie, K., Stockdon, H., Nordstrom, K., 2016. Dune management challenges on developed coasts. Shore Beach 84, 15–28.
Elko, N., Dietrich, C., Cialone, M., Stockdon, H., Bilskie, M.W., Boyd, B., Charbonneau, B.R., Cox, D., Dresback, K., Elgar, S., et al., 2019. Advancing the understanding of storm processes and impacts. Shore Beach 87, 37–51.
Feagin, R.A., Wu, X.B., Smeins, F.E., Whisenant, S.G., Grant, W.E., 2005. Individual versus community level processes and pattern formation in a model of sand dune plant succession. Ecol. Model. 183, 435–449.
Feagin, R.A., Figlus, J., Zinnert, J.C., Sigren, J., Martínez, M.L., Silva, R., Smith, W.K., Cox, D., Young, D.R., Carter, G., 2015. Going with the flow or against the grain? The promise of vegetation for protecting beaches, dunes, and barrier islands from erosion. Front. Ecol. Environ. 13, 203–210.
Fei, S., Phillips, J., Shouse, M., 2014. Biogeomorphic impacts of invasive species. Annu. Rev. Ecol. Evol. Syst. 45, 69–87.
Figlus, J., Kobayashi, N., Gralher, C., Iranzo, V., 2011. Wave overtopping and overwash of dunes. J. Waterw. Port Coast. Ocean Eng. 137, 26–33.
Food and Agriculture Organization of the United Nations (FAO), 1998. Crop evapotranspiration - Guidelines for computing crop water requirements - FAO Irrigation and drainage paper 56. Annex 2. Meteorological Tables. http://www.fao.org/docrep/x0490e/x0490e0j.html. (Accessed 4 December 2019).
Fordham, A.J., 1983. Of birds and bayberries: seed dispersal and propagation of three Myrica species. Arnoldia. 43 (4), 20–23.
Forster, S.M., Nicolson, T.H., 1981. Aggregation of sand from a maritime embryo sand dune by microorganisms and higher plants. Soil Biol. Biochem. 13, 199–203.
Franks, S.J., 2003. Facilitation in multiple life-history stages: evidence for nucleated succession in coastal dunes. Plant Ecol. 168, 1–11.
Gares, P.A., 1992. Topographic changes associated with coastal dune blowouts at island beach state park, New Jersey. Earth Surf. Process. Landf. 17, 589–604.
Gifford, R.M., 2003. Plant respiration in productivity models: conceptualization, representation and issues for global terrestrial carbon-cycle research. Funct. Plant Biol. 30, 171–186.
Godfrey, P.J., 1977. Climate, Plant Response and Development of Dunes on Barrier Beaches Along the U.S. East Coast. 21, pp. 203–216.
Goldstein, E.B., Mullins, E.V., Moore, L.J., Biel, R.G., Brown, J.K., Hacker, S.D., Jay, K.R., Mostow, R.S., Ruggiero, P., Zinnert, J.C., 2018. Literature-based latitudinal distribution and possible range shifts of two US east coast dune grass species (Uniola paniculata and Ammophila breviligulata). PeerJ 6 e4932–21.
Gombos, Z., Wada, H., Hideg, E., Murata, N., 1994. The unsaturation of membrane lipids stabilizes photosynthesis against heat stress. Plant Physiol. 104, 563–567.
Goudriaan, J., 1986. A simple and fast numerical method for the computation of daily totals of crop photosynthesis. Agric. For. Meteorol. 38, 249–254.
Goudriaan, J., van Laar, H.H., 1994. Modelling Potential Crop Growth Processes: Textbook with Exercises. Kluwer Academic Publishers, Dordrecht, The Netherlands.
Griffiths, M.E., 2006. Salt spray accumulation and heathland plant damage associated with a dry tropical storm in Southern New England. J. Coast. Res. 226, 1417–1422.
Griffiths, M.E., Orians, C.M., 2003. Responses of common and successional heathland species to manipulated salt spray and water availability. Am. J. Bot. 90, 1720–1728.
Hacker, S.D., Zarnetske, P., Seabloom, E., Ruggiero, P., Mill, J., Gerrity, S., Jones, C., 2011. Subtle differences in two non-native congeneric beach grasses significantly affect their colonization, spread, and impact. Oikos 121, 138–148.
Hacker, S.D., Jay, K.R., Cohn, N., Goldstein, E.B., Hovenga, P.A., Itzkin, M., Moore, L.J., Mostow, R.S., Mullins, E.V., Ruggiero, P., 2019. Species-specific functional morphology of four US Atlantic coast dune grasses: biogeographic implications for dune shape and coastal protection. Diversity 11 82–16.
Hamby, D.M., 1994. A review of techniques for parameter sensitivity analysis of environmental models. Environ. Monit. Assess. 32, 135–154.
Harman, B.P., Heyenga, S., Taylor, B.M., Fletcher, C.S., 2015. Global lessons for adapting coastal communities to protect against storm surge inundation. J. Coast. Res. 314, 790–801.
Hauer, M.E., Evans, J.M., Mishra, D.R., 2016. Millions projected to be at risk from sea-level rise in the continental United States. Nat. Clim. Chang. 1–8.
Hauser, A.S., 2006. Morella pensylvanica. Fire Effects Information System. U.S. Department of Agriculture, Forest Service, Rocky Mountain Research Station, Fire Sciences Laboratory . https://www.fs.fed.us/database/feis/plants/shrub/morpen/all.html. (Accessed 4 December 2019).
Hesp, P.A., 1984. The formation of sand beach ridges and foredunes. Spat. Accuracy 15, 289–291.
Hesp, P.A., 1989. A review of biological and geomorphological processes involved in the initiation and development of incipient foredunes. International Association for Scientific Hydrology 54, 181–201.

Hesp, P.A., Dong, Y., Cheng, H., Booth, J.L., 2019. Wind flow and sedimentation in artificial vegetation: Field and wind tunnel experiments. Geomorphology 337, 165–182.
Hester, M.W., McKee, K.L., Burdick, D.M., 1994. Clonal integration in Spartina patens across a nitrogen and salinity gradient. J. Bot. 72, 767–770.
Hodgson, D., McDonald, J.L., Hosken, D.J., 2015. What do you mean, 'resilient'? Trends Ecol. Evol. 30, 503–506.
Homer, C.G., Dewitz, J.A., Yang, L., Jin, S., Danielson, P., Xian, G., Coulston, J., Herold, N.D., Wickham, J.D., Megown, K., 2015. Completion of the 2011 National Land Cover Database for the conterminous United States-Representing a decade of land cover change information. Photogramm. Eng. Remote. Sens. 81 (5), 345–354.
Hoonhout, B.M., de Vries, S., 2016. A process-based model for aeolian sediment transport and spatiotemporal varying sediment availability. J. Geophys. Res. Earth Surf. 121, 1555–1575.
Houser, C., Hamilton, S., 2009. Sensitivity of post-hurricane beach and dune recovery to event frequency. Earth Surf. Process. Landf. 34, 613–628.
Houser, C., Hapke, C., Hamilton, S., 2008. Controls on coastal dune morphology, shoreline erosion and barrier island response to extreme storms. Geomorphology 100, 223–240.
Huang, H., Zinnert, J.C., Wood, L.K., Young, D.R., D'Odorico, P., 2018. Non-linear shift from grassland to shrubland in temperate barrier islands. Ecology 99, 1671–1681.
Huiskes, A.H.L., 1979. Ammophila Arenaria (L.) link (Psamma Arenaria (L.) Roem. Et Schult.; Calamgrostis Arenaria (L.) Roth). Aust. J. Ecol. 67, 363–382.
IPCC, 2014. In: Team, Core Writing, Pachauri, R.K., Meyer, L.A. (Eds.), Climate Change 2014: Synthesis Report. Contribution of Working Groups I, II and III to the Fifth Assessment Report of the Intergovernmental Panel on Climate Change. IPCC, Geneva, Switzerland 151 pp.
IPCC, 2019. Summary for policymakers. In: Pörtner, H.-O., Roberts, D.C., Masson-Delmotte, V., Zhai, P., Tignor, M., Poloczanska, E., Mintenbeck, K., Alegría, A., Nicolai, M., Okem, A., Petzold, J., Rama, B., Weyer, N.M. (Eds.), IPCC Special Report on the Ocean and Cryosphere in a Changing Climate.
Jackson, N.L., Nordstrom, K.F., 2018. Aeolian sediment transport on a recovering storm-eroded foredune with sand fences. Earth Surf. Process. Landf. 43, 1310–1320.
Jackson, N.L., Nordstrom, K.F., 2019. Trends in research on beaches and dunes on sandy shores, 1969-2019. Geomorphology 1–13.
Jackson, D.W.T., Costas, S., González-Villanueva, R., Cooper, A., 2019. A global 'greening' of coastal dunes_ an integrated consequence of climate change? Glob. Planet. Chang. 182, 103026.
Jennings, S., 2004. Coastal tourism and shoreline management. Ann. Tour. Res. 31 (4), 899–922.
Johnson, B.D., Kobayashi, N., Gravens, M.B., 2012. Cross-Shore Numerical Model CSHORE for Waves, Currents, Sediment Transport and Beach Profile Evolution. Engineer Research and Development Center, Coastal and Hydraulics Lab, Vicksburg, Mississippi No. ERDC/CHL-TR-12-22, 158p.
Jones, C.G., Lawton, J.H., Shachak, M., 1994. Organisms as ecosystem engineers. Oikos 69, 373–386.
Keijsers, J.G.S., De Groot, A.V., Riksen, M.J.P.M., 2015. Vegetation and sedimentation on coastal foredunes. Geomorphology 228, 723–734.
Keijsers, J., De Groot, A.V., Riksen, M.J.P.M., 2016. Modeling the biogeomorphic evolution of coastal dunes in response to climate change. Journal of Geophysical Research Earth Surface 121, 1161–1181.
Kluepfel, M., Polomski, B., 2015. Wax Myrtle Factsheet. Clemson University Cooperative Extension Home & Garden Information Center. https://hgic.clemson.edu/factsheet/waxmyrtle. (Accessed 1 July 2020).
Kobayashi, N., Gralher, C., Do, K., 2013. Effects of Woody Plants on Dune erosion and Overwash. J. Waterw. Port Coast. Ocean Eng. 139 (6), 466–472.
Konlechner, T.M., Hilton, M.J., Orlovich, D.A., 2013. Accommodation space limits plant invasion: Ammophila arenaria survival on New Zealand beaches. J. Coast. Conserv. 17, 463–472.
Lazarus, E.D., Armstrong, S., 2015. Self-organized pattern formation in coastal barrier washover deposits. Geology 43, 363–366.
Leatherman, S.P., Zhang, K., Douglas, B.C., 2000. Sea level rise shown to drive coastal erosion. Eos 81, 55–57.
Li, F., van Gelder, P.H.A.J.M., Vrijling, J.K., Callaghan, D.P., Jongejan, R.B., Ranasinghe, R., 2014. Probabilistic Estimation of Coastal Dune Erosion and Recession by Statistical Simulation of Storm Events. 47. Elsevier, 53, pp. 53–62.
Lindell, J., Fredriksson, C., Hanson, H., 2017. Impact of dune vegetation on wave and wind erosion: a case study at Ängelholm Beach, South Sweden. J. Water Manag. Res. 73, 39–48.
Little, L.R., Maun, M.A., 1996. The 'Ammophila problem' revisited: a role for mycorrhizal fungi. J. Ecol. 84, 1–7.
Liu, Q.Q., Singh, V.P., 2004. Effect of microtopography, slope length and gradient, and vegetative cover on overland flow through simulation. J. Hydrol. Eng. 9 (5), 375–382.
Lonard, R.I., Judd, F.W., Staltler, R., 2010. The biological flora of coastal dune and wetlands: Spartina patens. J. Coast. Res. 26, 935–946.
Luna, M.C.D.M., Parteli, E.J., Durán, O., Herrmann, H.J., 2011. Model for the genesis of coastal dune fields with vegetation. Geomorphology 129 (3-4), 215–224.
Mardhiah, U., Caruso, T., Gurnell, A., Rillig, M.C., 2016. Arbuscular mycorrhizal fungal hyphae reduce soil erosion by surface water flow in a greenhouse experiment. Appl. Soil Ecol. 99, 137–140.
Martin, W.E., 1959. The vegetation of island-beach-state-park, New-Jersey. Ecol. Monogr. 29, 1–46.
Martinez, M.L.M., Moreno-Casasola, P., 1996. Effects of burial by sand on seedling growth and survival in six tropical sand dune species from the Gulf of Mexico. J. Coast. Res. 12, 406–419.
MathWorks, Inc, 2018. MATLAB and Statistics and Machine Learning Toolbox Release 2018a. The MathWorks, Inc, Natick, Massachusetts, United States.
Maun, M.A., 1985. Population biology of Ammophila breviligulata and Calamovilfa longifolia on Lake Huron sand dunes. I. Habitat, growth form, reproduction, and establishment. Can. J. Bot. 63, 113–124.
Maun, M.A., 1998. Adaptations of plants to burial in coastal sand dunes. Can. J. Bot. 76, 713–738.
Maun, M.A., 2009. The Biology of Coastal Sand Dunes. Oxford University Press, Oxford, UK.
Maun, M.A., Lapierre, J., 1986. Effects of burial by sand on seed germination and seedling emergence of four dune species. Am. J. Bot. 73, 450–455.
Maun, M.A., Perumal, J.V., 1999. Zonation of vegetation on lacustrine coastal dunes: effects of burial by sand. Ecol. Lett. 2, 14–18.
Miller, D.L., Thetford, M., Schneider, M., 2008. Distance from the gulf influences survival and growth of three barrier island dune plants. J. Coast. Res. 4, 261–266.
Moore, L.J., Durán Vinent, O., Ruggiero, P., 2016. Vegetation control allows autocyclic formation of multiple dunes on prograding coasts. Geology G37778, 1–4.
Moreno-Casasola, P., 1986. Sand movement as a factor in the distribution of plant communities in as coastal dune system. Vegetatio 65, 67–76.
Morton, R.A., Paine, J.G., 1985. Beach and vegetation-line changes at Galveston Island, Texas. Erosion, deposition, and recovery from Hurricane Alicia. Bureau of Economic Geology Geological Circular 85.
Mulder, C., Hendriks, A.J., 2014. Half-saturation constants in functional responses. Glob. Ecol. Conserv. 2, 161–169.
Mullins, E., Moore, L.J., Goldstein, E.B., Jass, T., Bruno, J., Durán Vinent, O., 2019. Investigating dune-building feedback at the plant level: insights from a multispecies field experiment. Earth Surf. Process. Landf. 60, 205–214.
Murray, A.B., 2007. Reducing model complexity for explanation and prediction. Geomorphology 90 (3–4), 178–191.
van Nes, E.H., Scheffer, M., van den Berg, M.S., Coops, H., 2003. Charisma: a spatial explicit simulation model for submerged macrophytes. Ecol. Model. 150, 103–116.
Nield, J.M., Baas, A.C.W., 2008. Investigating parabolic and nebkha dune formation using a cellular automaton modelling approach. Earth Surf. Process. Landf. 33, 724–740.
Noble, I.R., Weiss, P.W., 1989. Movement and modelling of buried seed of the invasive perennial Chrysanthemoides monilifera in coastal dunes and biological control. Aust. J. Ecol. 14, 55–64.
Nordstrom, K.F., Jackson, N.L., 1993. The role of wind direction in eolian transport on a narrow sandy beach. Earth Surf. Process. Landf. 18, 675–685.
OCM Partners, 2020a. 2017. USACE NCMP Topobathy Lidar DEM: East Coast (NY, NJ, DE, MD, VA, NC, SC, GA) from 2010-06-15 to 2010-08-15. NOAA National Centers for Environmental Information. https://www.fisheries.noaa.gov/inport/item/52446. (Accessed October 2020).
OCM Partners, 2020b. CoNED Topobathymetric Model for New Jersey and Delaware, 1880 to 2014 from 2010-06-15 to 2010-08-15. NOAA National Centers for Environmental Information. https://www.fisheries.noaa.gov/inport/item/49467. (Accessed October 2020).
Okin, G.S., 2008. A new model of wind erosion in the presence of vegetation. J. Geophys. Res. Earth Surf. 113, F02S10.
Rastetter, E.B., 1991. A spatially explicit model of vegetation-habitat interactions on barrier islands. In: Turner, M.G., Gardener, R.H. (Eds.), Quantitative Methods in Landscape Ecology. Springer-Verlag, New York, pp. 353–358.
van Rijn, L.C., 2009. Prediction of dune erosion due to storms. Coast. Eng. 56, 441–457.
Roelvink, D., Reniers, A., van Dongeren, A., 2009. Modelling storm impacts on beaches, dunes and barrier islands. Coast. Eng. 56, 1133–1152.
Roelvink, D., Reniers, A.J.H.M., Van Dongeren, A., Van Thiel de Vries, J., Lescinski, J., & McCall, R., 2010. XBeach model description and manual. Unesco-IHE Institute for Water Education, Deltares and Delft University of Technology Report. June, 21, 2010.
Roelvink, D., Costas, S., 2019. Coupling nearshore and aeolian processes: XBeach and DUNA process-based models. Environ. Model. Softw. 115, 98–112.
Sallenger Jr., A.H., 2000. Storm impact scale for barrier islands. J. Coast. Res. 16, 890–895.
Scheffer, M., Baveco, J.M., DeAngelis, D.L., Rose, K.A., van Nes, E.H., 1995. Super-individuals a simple solution for modelling large populations on an individual basis. Ecol. Model. 80, 161–170.
Schoonees, T., Gijón Mancheño, A., Scheres, B., Bouma, T.J., Silva, R., Schlurmann, T., Schüttrumpf, H., 2019. Hard Structures for Coastal Protection, Towards Greener designs. Estuar. Coasts 42, 1709–1729.
Sharkey, T.D., 2005. Effects of moderate heat stress on photosynthesis: importance of thylakoid reactions, rubisco deactivation, reactive oxygen species, and thermotolerance provided by isoprene. Plant Cell Environ. 28, 269–277.
Sharp, W.C., Hawk, V.B., 1977. Establishment of Woody Plants for Secondary and Tertiary Dune Stabilization Along the Mid-Atlantic Coast.
Slaymaker, D.H., Peek, M.S., Wresilo, J., Zeltner, D.C., Saleh, Y.F., 2015. Genetic Structure of Native and Restored Populations of American Beachgrass (Ammophila breviligulata Fern.) along the New Jersey Coast. J. Coast. Res. 316, 1334–1343.
Spendelow, J.A., Nichols, J.D., Hines, J.E., Lebreton, J.D., Pradel, R., 2002. Modelling postfledging survival and age-specific breeding probabilities in species with delayed maturity: a case study of Roseate Terns at Falkner Island, Connecticut. J. Appl. Stat. 29, 385–405.
Stallins, J.A., 2005. Stability domains in barrier island dune systems. Ecol. Complex. 2, 410–430.
Stallins, J.A., 2006. Geomorphology and ecology: Unifying themes for complex systems in biogeomorphology. Geomorphology 77, 207–216.
Stallins, J.A., Corenblit, D., 2018. Interdependence of geomorphic and ecologic resilience properties in a geographic context. Geomorphology 305, 76–93.
Tahiri, A.Z., Yasuda, H.A.H., 2006. Fixed and variable light extinction coefficients for estimating plant transpiration and soil evaporation under irrigated maize. Agric. Water Manag. 84 (1–2), 186–192.

Tanaka, N., Nandasena, N.A.K., Jinadasa, K.B.S.N., Sasaki, Y., Tanimoto, K., Mowjood, M.I.M., 2009. Developing effective vegetation bioshield for tsunami protection. Civ. Eng. Environ. Syst. 26, 163–180.

Teh, C.B.S., 2006. Introduction to Mathematical Modeling of Crop Growth: How the Equations are Derived and Assembled Into a Computer Model. Brown Walker Press, Boca Raton, Florida.

Thornley, J.H.M., 2011. Plant growth and respiration re-visited: maintenance respiration defined – it is an emergent property of, not a separate process within, the system – and why the respiration : photosynthesis ratio is conservative. Ann. Bot. 108, 1365–1380.

Treshow, M., Harper, K., 1974. Longevity of perennial forbs and grasses. Oikos 25, 93–96.

Tyndall, R.W., Levy, G.F., 1978. Plant distribution and succession within interdunal depressions on a Virginia barrier dune system. J. Elisha Mitchell Sci. Soc. 94, 1–15.

Uva, R.H., 2003. Growth and Yield of Beach Plum (Prunus maritima Marshall) in Horticultural, Land Restoration, and Ecological Systems. Cornell University Doctoral Dissertation.

Van der Zande, D., Stuckens, J., Verstraeten, W.W., Muys, B., Coppin, P., 2010. Open AccessArticle Assessment of Light Environment Variability in Broadleaved Forest Canopies using Terrestrial Laser Scanning. Remote Sens. 2, 1564–1574.

Van Oijen, M., Schapendonk, A., Höglind, M., 2010. On the relative magnitudes of photosynthesis, respiration, growth and carbon storage in vegetation. Ann. Bot. 105, 793–797.

Viles, H., 2020. Biogeomorphology: past, present and future. Geomorphology 366, 106809–106815.

Vogel, R.M., Castellarin, A., 2017. Risk, reliability, and return periods and hydrologic design. In: Singh, V.P. (Ed.), Handbook of Applied Hydrology. McGraw-Hill Book Company, New York, NY, USA.

Walker, I.J., Davidson-Arnott, R.G.D., Bauer, B.O., Hesp, P.A., Delgado-Fernandez, I., Ollerhead, J., Smyth, T.A.G., 2017. Scale-dependent perspectives on the geomorphology and evolution of beach-dune systems. Earth Sci. Rev. 171, 220–253.

Wang, M., White, N., Grimm, V., Hofman, H., Doley, D., Thorp, G., Cribb, B., Wherritt, E., Han, L., Wilkie, J., et al., 2018. Pattern-oriented modelling as a novel way to verify and validate functional–structural plant models: a demonstration with the annual growth module of avocado. Ann. Bot. 121, 941–959.

Webb, J.W., Dodd, J.D., Koerth, B.H., Weichert, A.T., 1984. Seedling Establishment of Spartina alterniflora and Spartina patens on Dredged Materials in Texas. Gulf Research Reports 7, 1–6.

Wernette, P., Houser, C., Bishop, M.P., 2016. An automated approach for extracting Barrier Island morphology from digital elevation models. Geomorphology 262, 1–7.

Wernette, P., Thompson, S., Eyler, R., Taylor, H., Taube, C., Medlin, A., Decuir, C., Houser, C., 2018. Defining dunes: evaluating how dune feature definitions affect dune interpretations from remote sensing. J. Coast. Res. 34, 1460–1470.

de Winter, R.C., Gongriep, F., Ruessink, B.G., 2015. Observations and modeling of alongshore variability in dune erosion at Egmond aan Zee, the Netherlands. Coast. Eng. 99, 167–175.

de Wit, C.T., 1965. Photosynthesis of leaf canopies. Agricultural Research Reports 663. Pudoc, Wageningen.

Wolner, C.W.V., Moore, L.J., Young, D.R., Brantley, S.T., Bissett, S.N., McBride, R.A., 2013. Ecomorphodynamic feedbacks and barrier island response to disturbance: Insights from the Virginia Barrier Islands, Mid-Atlantic Bight, USA. Geomorphology 199, 115–128.

Woodhouse Jr., W.W., 1982. Coastal sand dunes of the U.S. In: Lewis III, R.R. (Ed.), Creation and Restoration of Coastal Plant Communities. Boca Raton, FL, pp. 1–44 e4932–21.

Wootton, L., Miller, J., Miller, C., Peek, M., Williams, A., Rowe, P., 2016. NJ Sea Grant Consortium Dune Manual.

Wright, C.W., Troche, R.J., Kranenburg, C.J., Klipp, E.S., Fredericks, Xan, Nagle, D.B., 2014. EAARL-B submerged topography—Barnegat Bay, New Jersey, post-Hurricane Sandy, 2012–2013: U.S. Geological Survey Data Series 887. https://doi.org/10.3133/ds887. (Accessed 26 August 2020).

Young, D.R., Brantley, S.T., Zinnert, J.C., Vick, J.K., 2011. Landscape position and habitat polygons in a dynamic coastal environment. Ecosphere 2 (1–15), 71.

Yuan, T., Maun, M.A., Hopkins, W.G., 1993. Effects of sand accretion on photosynthesis, leaf-water potential and morphology of two dune grasses. Funct. Ecol. 7, 676–682.

Zarnetske, P.L., Hacker, S.D., Seabloom, E.W., Ruggiero, P., Killian, J.R., Maddux, T.B., Cox, D., 2012. Biophysical feedback mediates effects of invasive grasses on coastal dune shape. Ecology 93, 1439–1450.

Zhang, W., Schneider, R., Kolb, J., Teichmann, T., Dudzinska-Nowak, J., Harff, J., Hanebuth, T.J.J., 2015. Land–sea interaction and morphogenesis of coastal foredunes — a modeling case study from the southern Baltic Sea coast. Coast. Eng. 99, 148–166.